

Science of the Total Environment

Earthquake, floods and changing land use history: a 200-year overview of environmental changes in southern Siberia as indicated by n-alkanes and related proxies in sediments from shallow lakes

--Manuscript Draft--

Manuscript Number:	
Article Type:	Research Paper
Keywords:	sedimentary organic matter; molecular biomarkers; isoprenoids; Selenga River basin; environmental changes.
Corresponding Author:	Cesar C Martins, Dr. Federal University of Parana Pontal do Parana, PR, BRAZIL
First Author:	Cesar C Martins, Dr.
Order of Authors:	Cesar C Martins, Dr. Jennifer K Adams, PhD Handong Yang, PhD Alexander A Shchetnikov, PhD Maikon Di Domenico, PhD Neil Rose, PhD Anson Mackay, PhD
Abstract:	<p>The Selenga River basin, located in southern Siberia, is an important component of the Lake Baikal ecosystem, and comprises approximately 80% of the Baikal watershed. The Selenga Delta, is one of the largest inland freshwater floodplains in the world, and plays an important role in the ecosystem functioning of Baikal. The Lake Gusinoye region, is southwest of Lake Baikal and the Selenga Delta, is a more heavily industrialized region within the Selenga River basin. We assessed possible drivers of changes of sedimentary organic matter (OM) composition within two shallow lakes. We focused on individual n-alkanes, one of the most abundant lipids used to provide information on past vegetation. We used multivariate statistics to disentangle changes in the sources of sedimentary OM over time. The depositional OM history of SLNG04B core can be divided in four zones: (i) major influence of non-emergent vascular plants, typically found in transitional environments (ca. 1835 to ca. 1875); (ii) increased influence of grasses/herbs (ca. 1880 to ca. 1910); (iii) transition from non-emergent vascular plants and grasses/herbs to submerged and floating macrophytes and phytoplankton (ca. 1915 to ca. 1945); (iv) maintenance of autochthonous OM from submerged and floating macrophytes and phytoplankton (ca. 1945 to ca. 2014). The depositional OM history of the Black Lake core can be divided in two main zones: (i) major influence of non-emergent vascular plants and submerged and floating macrophytes (ca. 1915 to ca. 1980); (ii) increased influence of grasses/herbs and phytoplankton (ca. 1980 to ca. 2010). Natural events (e.g., an earthquake in 1862 caused flooding and subsidence of much of the land surrounding SLNG04 lake and a further catastrophic flood event in 1897) and anthropogenic activities (e.g., nutrient pollution from expansion of agricultural) changed the composition of OM resulting in ecological shifts across trophic levels in the Selenga River basin.</p>
Suggested Reviewers:	Ana Cecília Rizzatti de Albergaria Barbosa, PhD Federal University of Bahia cecilia.albergaria@ufba.br Specialist in organic biomarkers (n-alkanes) from aquatic environments P Harding, PhD poppy.harding@rhul.ac.uk Author: Global and Planetary Change 195 (2020) 103333 - Manuscript about Southern Siberia

	<p>G.L.B. Wiesenberg, PhD guido.wiesenberg@geo.uzh.ch Author of Quaternary International 365 (2015) 190-202 about lipid biomarkers and Siberia</p>
	<p>Loeka L Jongejans, PhD Loeka.jongejans@awi.de Author of "n-Alkane Characteristics of Thawed Permafrost Deposits Below a Thermokarst Lake on Bykovsky Peninsula, Northeastern Siberia" Front. Environ. Sci. 8:118. doi: 10.3389/fenvs.2020.00118</p>
	<p>Suzanne McGowan, PhD S.McGowan@nioo.knaw.nl</p> <p>She is an organic geochemist and has worked on Lake Baikal</p>
	<p>David Ryves, PhD Loughborough University d.b.ryves@lboro.ac.uk He has a diatom and stable isotope expert, but has knowledge of Baikal ecosystems</p>
<p>Opposed Reviewers:</p>	



Pontal do Paraná, December 15, 2022

To: Editor-in-Chief – *Science of the Total Environment*

Dear Editor-in-Chief

We would like to submit the enclosed manuscript, entitled “*Earthquake, floods and changing land use history: a 200-year overview of environmental changes in southern Siberia as indicated by n-alkanes and related proxies in sediments from shallow lakes*” for your consideration for possible publication in *Science of the Total Environment*.

The study assessed the temporal variability of sedimentary organic matter (OM) composition and inputs to two shallow water bodies within the Selenga River basin, an important component of the Lake Baikal ecosystem, classified as a UNESCO World Heritage site as well as a Ramsar site, designated for the conservation and sustainable development of wetlands throughout the world. In this study, sedimentary *n*-alkanes, one of the most common lipids used to provide information on past vegetation, were used to indicate historical changes in the ecological structure of these shallow lakes.

We found that natural events (e.g., an earthquake in 1862 which caused flooding and subsidence around one of the studied lakes and a further catastrophic flood event in 1897) and anthropogenic activities (e.g., nutrient pollution from expansion of agricultural and livestock population) changed the composition of sedimentary OM at the lakes resulting in ecological shifts across trophic levels in the Selenga River basin. These events were well characterized using *n*-alkanes, and confirmed by other sedimentary proxies (e.g., diatoms, microfossils), emphasising the linkages between these waterbodies, their connectivity to the Selenga River and the changing use of the terrestrial landscape within their catchments.

The shallow lake systems of the Selenga River basin are of critical importance in maintaining the ecosystem health of Lake Baikal and may act as sentinels for recent environmental change. Given the importance of Lake Baikal to the Siberian environment, the protection of its ecosystems is a global concern, especially as recent reports indicate increased accumulation of a variety of contaminants and dramatic changes in the deltaic environment due to global warming. Our study uses organic biomarkers to provide a novel assessment of sedimentary OM dynamics in freshwater floodplain wetlands, as well as a greater understanding of how local environmental changes impact these systems on spatial and temporal scales. As a consequence, we believe it will be of great interest to the broad readership of *Science of the Total Environment*.

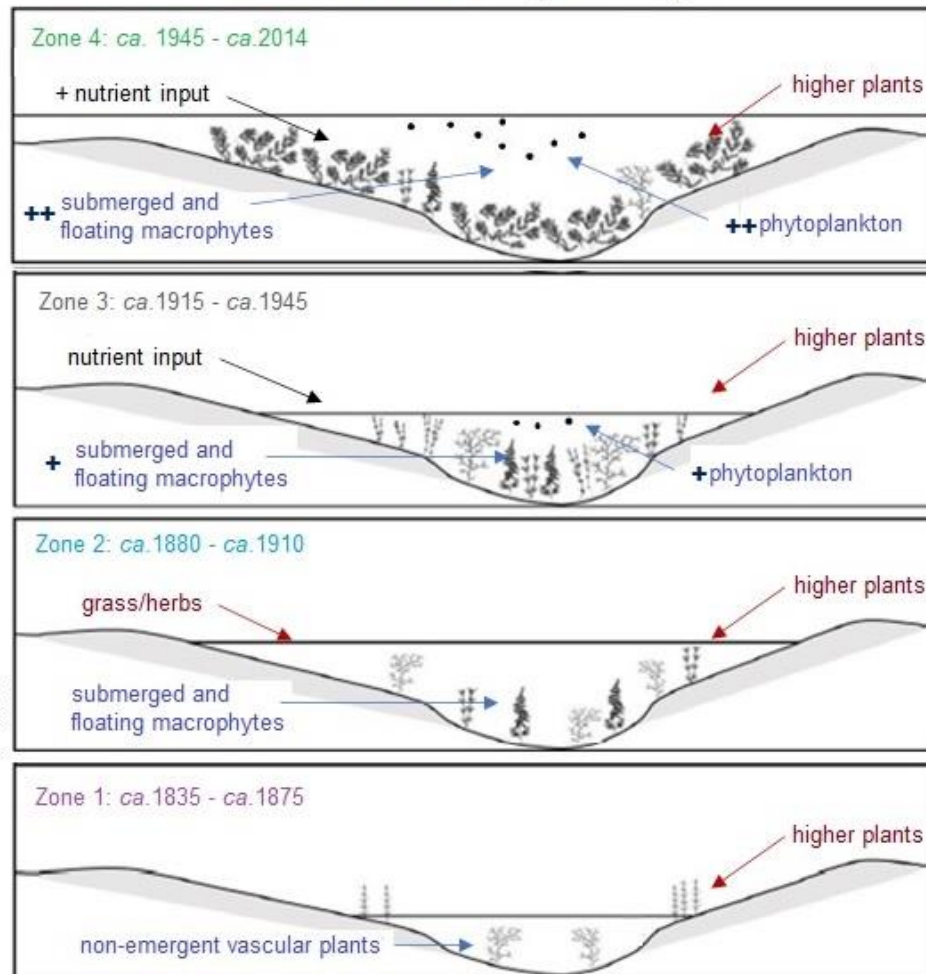
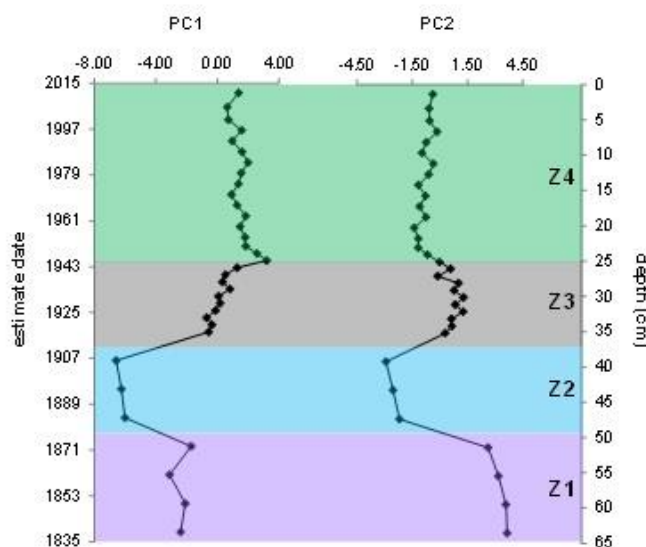
Yours sincerely,

Prof. Dr. César de Castro Martins
Centro de Estudos do Mar - UFPR
<http://orcid.org/0000-0002-2515-5565>

Graphical Abstract



SLNG4 Lake - the Selenga Delta region



Highlights

- > Secular variability on sedimentary organic matter from Siberian lakes is presented
- > *n*-alkanes and multivariate data show ecological changes in Siberian lakes
- > Changes on sedimentary organic matter are both natural and anthropogenically-induced
- > Nutrients from agriculture and livestock changed inputs of sedimentary OM over time

[Click here to view linked References](#)

1 **Earthquake, floods and changing land use history: a 200-year overview of environmental**
2 **changes in southern Siberia as indicated by *n*-alkanes and related proxies in sediments from**
3 **shallow lakes**

4
5 César C. Martins ^{a,b,*}, Jennifer K. Adams ^{b,c,*}, Handong Yang ^b, Alexander A. Shchetnikov ^{d,e,f},
6 Maikon Di Domenico ^a, Neil L. Rose ^b, Anson W. Mackay ^b

7
8 ^a Centro de Estudos do Mar, Campus Pontal do Paraná, Universidade Federal do Paraná, Caixa
9 Postal 61, 8325-976 Pontal do Paraná, PR, Brazil.

10 ^b Environmental Change Research Centre, Department of Geography, University College London,
11 Gower Street, London, WC1E 6BT, UK.

12 ^c Biology Department, University of Waterloo, 200 University Avenue West, Waterloo, ON, N2L
13 3G1, Canada.

14 ^d Institute of the Earth's Crust, Siberian Branch of the Russian Academy of Sciences, Irkutsk,
15 664033, Russia.

16 ^e Vinogradov Institute of Geochemistry, Siberian Branch of Russian Academy of Sciences,
17 Irkutsk, 664033, Russia.

18 ^f Irkutsk Scientific Center, Siberian Branch of the Russian Academy of Sciences, Irkutsk, 664033,
19 Russia.

20

21 **Corresponding authors:** ccmart@ufpr.br (C.C. Martins)

22 j24adams@uwaterloo.ca (J.K. Adams)

23 **Abstract**

24 The Selenga River basin, located in southern Siberia, is an important component of the Lake Baikal
25 ecosystem, and comprises approximately 80% of the Baikal watershed. Within the Selenga River
26 basin, two localized study regions were chosen. The first, the Selenga Delta, is one of the largest
27 inland freshwater floodplains in the world, and plays an important role in the ecosystem
28 functioning of Baikal. It purifies the river waters before they enter the lake, and acts as a refuge
29 for many of Baikal's endemic species. The second location, the Lake Gusinoe region, is
30 southwest of Lake Baikal and the Selenga Delta, and was chosen as a more heavily industrialized
31 region within the Selenga River basin. Anthropogenic activities, including industry, urban
32 settlements, aquaculture and agriculture, have historically increased ecological damage within this
33 area. We assessed possible drivers of changes of sedimentary organic matter (OM) composition
34 within two shallow lakes (SLNG04 and Black Lake), located in the Selenga Delta and the Selenga
35 watershed, respectively. We focused on individual *n*-alkanes, one of the most abundant and
36 common lipids used to provide information on past vegetation. We used multivariate statistics to
37 disentangle changes in the sources of sedimentary OM over time. The depositional OM history of
38 SLNG04B core can be divided in four zones: (i) major influence of non-emergent vascular plants,
39 typically found in transitional environments (*ca.* 1835 to *ca.* 1875); (ii) increased influence of
40 grasses/herbs (*ca.* 1880 to *ca.* 1910); (iii) transition from non-emergent vascular plants and
41 grasses/herbs to submerged and floating macrophytes and phytoplankton (*ca.* 1915 to *ca.* 1945);
42 (iv) maintenance of autochthonous OM from submerged and floating macrophytes and
43 phytoplankton (*ca.* 1945 to *ca.* 2014). The depositional OM history of the Black Lake core can be
44 divided in two main zones: (i) major influence of non-emergent vascular plants and submerged
45 and floating macrophytes (*ca.* 1915 to *ca.* 1980); (ii) increased influence of grasses/herbs and
46 phytoplankton (*ca.* 1980 to *ca.* 2010). Natural events (e.g., an earthquake in 1862 caused flooding
47 and subsidence of much of the land surrounding SLNG04 lake and a further catastrophic flood

48 event in 1897) and anthropogenic activities (e.g., nutrient pollution from expansion of agricultural
49 and livestock population) changed the composition of sedimentary OM resulting in ecological
50 shifts across trophic levels in the Selenga River basin.

51

52 **Keywords:** sedimentary organic matter; molecular biomarkers; isoprenoids; Selenga River basin;
53 environmental changes.

54 **1. Introduction**

55 Freshwater floodplain wetlands are some of the most dynamic, diverse, productive and
56 often complex ecosystems on Earth, occurring most extensively in regions where precipitation
57 exceeds evapotranspiration (Mitsch and Gosselink, 2007). They are characterized by regularly
58 flooded land, a highly connective landscape, and shallow lakes of varying degrees of connectivity
59 (Junk et al., 2013). More than 80% of known inland wetland systems have been historically lost,
60 especially during the late 20th century (Davidson et al., 2018; Wasserman and Dalu, 2022), due to,
61 e.g., nutrient enrichment from urban and agricultural sources, the construction of dams, stream
62 channelization and dredging for flood control (Hobbs et al., 2016; Sievers et al., 2018).

63 Climate-induced changes in the hydrological regime are often very important drivers of
64 organic matter (OM) production and ecological variability within freshwater wetlands, and
65 consequently, in the type of sedimentary OM accumulated in shallow lakes. They are also often
66 attributed to changes in precipitation levels, which can result in complete shifts in the vegetation
67 and ecological structure within the wetland resulting in different types of sedimentary OM
68 (Cobbaert et al., 2014; Levi et al., 2016). Therefore, the OM content of lake sediments provides a
69 variety of indicators that can be used to infer histories of environmental conditions of lakes and
70 their watersheds (Rullkötter, 2000; Pancost and Boot, 2004). The primary source of OM to lake
71 sediments is from plants in and around the lake. Plants can be divided into two geochemically
72 distinctive groups on the basis of their biochemical compositions: (1) non-vascular plants such as
73 phytoplankton (e.g., cyanobacteria, algae, diatoms, dinoflagellates) that contain little or no carbon-
74 rich cellulose and lignin, and (2) vascular plants, such as grasses, herbs, shrubs, trees on land, and
75 macrophytes in lakes, that contain large proportions of these tissues (Meyers and Teranes, 2001).

76 Biomarkers are a group of widespread geochemical compounds present in sedimentary OM
77 and applied in the (paleo)reconstruction of regional climate changes (Freeman and Pancost, 2014).
78 Biomarkers can distinguish between allochthonous and autochthonous carbon sources, and also

79 anthropogenic inputs based on differences in molecular types, functional group positions, and
80 carbon chain length (Derrien et al., 2017; Inglis et al., 2022). Biomarkers can also identify specific
81 types of OM sources over time (Volkman et al., 2008). Amongst biomarkers, *n*-alkanes are one of
82 the most common lipids used to provide information on past vegetation. They are biosynthesized
83 by terrestrial and aquatic higher plants and phytoplankton (Eglinton and Hamilton, 1967; Ficken
84 et al., 2000), and have odd-to-even dominance in the number of carbon atoms. Short carbon chain-
85 length *n*-alkanes ($< C_{20}$) are biosynthesized mainly by bacteria and phytoplankton (Derrien et al.,
86 2017; Liu et al., 2020) while submerged and floating macrophytes (classified as non-emergent
87 vascular plants) are generally dominated by medium-carbon chain-length *n*-alkanes (i.e., C_{20} - C_{25}).
88 Terrestrial sources are dominated by long-carbon chain-length *n*-alkanes ($> C_{25}$) and have a strong
89 odd-to-even carbon preference (Chen et al., 2016). As a component of vascular plant leaf wax, *n*-
90 alkane distribution is generally dominated by *n*- C_{27} to *n*- C_{35} , being more abundant in deciduous
91 trees/shrubs and biosynthesized by grasses/herbs (Schefuß et al., 2003).

92 The aim of this study was to assess the variability of sedimentary OM composition within
93 shallow water bodies of the Selenga Delta, a designated Ramsar site (N^o 682), for the conservation
94 and sustainable development of wetlands throughout the world (Ramsar, 2022), and nearby region
95 of the Selenga River basin. Anthropogenic activities within the Selenga River basin, including
96 industry, agriculture, aquaculture, growing urban settlements, mining, and deforestation, pose
97 threats to water quality and ecology in the Delta and other nearby catchment lakes through both
98 chemical pollution (Adams et al., 2018) and increased erosion of sediments into the Selenga river
99 (Bazhenova and Kohylkin, 2013). Two shallow lakes in the region were selected for biomarker
100 analysis (*n*-alkanes and their related ratios) to evaluate the temporal variations in the input and
101 sources of *n*-alkanes through the last decades. We also tried to answer a specific question: can
102 sedimentary *n*-alkanes be used to indicate changes in the ecological structure of Selenga River
103 basin shallow lakes?

104 **2. Study area**

105 *2.1. The Selenga River basin*

106 The Selenga River basin is located in the continental subarctic of southeast Siberia (Fig.
107 1), and covers an area of almost 450,000 km² in Siberia and Mongolia, comprising over 80% of
108 the Lake Baikal watershed (Nadmitov et al., 2015). The Selenga River flows approximately 950
109 km from the head waters in northern Mongolia before it reaches the Selenga Delta and Lake Baikal.
110 The upstream portions of the Selenga River basin, primarily tributaries and headwaters within
111 Mongolia, run through mountainous and forested terrain, while further downstream, the southern
112 Siberian portion, is dominated by steppe vegetation, underlain by permafrost. Part of this steppe
113 has been converted to pasture or crop land (Chalov et al., 2016). Peak river discharge occurs during
114 the summer, when 98% of total sediment loads are transported through the Selenga River basin
115 (Chalov and Romanchenko, 2016). The region is characterized by an ultracontinental climate, with
116 dry, intensely cold winters and short, mild summers, subjected to westerly and northwesterly winds
117 all year-round (Plyusnin et al., 2008).

118 The Selenga Delta itself (52°14'N; 106°30'E), has formed where the Selenga River enters
119 Lake Baikal, the oldest and deepest lake in the world and classified as a UNESCO World Heritage
120 since 1996. The delta is heavily influenced by tectonic processes with the oldest portions having
121 been formed over two to three million years ago (Scholz and Hutchinson, 2000).

122

123 *2.2. Sampled study sites*

124 Two shallow lakes were selected for study. The first is located within the Selenga Delta
125 itself ('SLNG04'; 52°16'N, 106°40'E), and the second, located outside of the Selenga Delta, but
126 within the Selenga River basin (named 'Black Lake'; 51°24'N, 106°29'E) (Fig. 2). SLNG 04 is
127 an expansive shallow lake, with surface flow connections to both the Selenga River and Lake
128 Baikal. It is partially surrounded by agricultural lands, consisting primarily of livestock rearing.

129 Black Lake is one in a chain of several shallow freshwater lakes located approximately 200 km
130 upstream of the Selenga Delta along the Selenga River, and 80 km direct distance southeast of
131 Lake Baikal (Pisarsky et al., 2005). Black Lake is situated in the more heavily industrialized area
132 of Gusinoye, and provides therefore a useful comparison to SLNG04.

133

134 **3. Material and Methods**

135 *3.1. Extraction of sediment cores*

136 In March 2014, sediment cores were extracted from SLNG04 and Black Lake ('SLNG04B'
137 and 'BRYT02B', respectively), for organic compound analyses. Further sediment cores
138 ('SLNG04C' and 'BRYT02C') were extracted at the same sites for radiometric dating analyses.
139 An Uwitec piston corer (UWITEC Ltd., Austria) fitted with a 6.3 cm internal diameter perspex
140 tube (*n*-hexane-cleaned to eliminate organic contamination) was used. Sediment cores were
141 collected while lakes were ice-covered, through an auger-drilled hole in the ice. Sediment from
142 these cores was vertically extruded and sliced at 0.5 cm intervals in the field, using *n*-hexane-
143 cleaned equipment and placed in *n*-hexane cleaned aluminum foil before being stored in a plastic
144 bag and sealed. Sediments were stored at -20°C and then freeze-dried in preparation for analysis.
145 Dried sediment from each sample depth was ground to a fine powder using an agate mortar and
146 pestle.

147

148 *3.2. Methods for radioisotope dating of sediment cores*

149 Radiometric dating techniques were used to date the SLNG04C and BRYT02C sediment
150 cores. The detailed methods were published in Adams et al. (2018). Briefly, wet sediment was
151 subsampled from sediment cores at 3.0-cm intervals and freeze-dried. Dried sediment samples
152 were analyzed for ^{210}Pb , ^{226}Ra , ^{137}Cs and ^{241}Am by direct gamma assay using ORTEC HPGe GWL
153 series well-type coaxial low background intrinsic germanium detectors. ^{210}Pb was determined via

154 its gamma emissions at 46.5keV, and ^{226}Ra by the 295keV and 352keV gamma rays emitted by its
155 daughter isotope ^{214}Pb . ^{210}Pb chronologies for both sediment cores were constructed using the
156 constant rate of supply (CRS) dating model (Appleby and Oldfield, 1978; Appleby, 2001).
157 Artificial radionuclides ^{137}Cs and ^{241}Am were measured by their emissions at 662keV and
158 59.5keV, respectively (Appleby et al., 1986). To obtain dates for the undated cores ('B') loss-on-
159 ignition at 550 °C (LOI₅₅₀) was conducted on all collected sediment cores (Heiri et al., 2001).
160 LOI₅₅₀ profiles from both 'B' and 'C' cores were examined for distinct features (i.e., tie-points)
161 present in profiles from both cores. The radiometric dates for the tie-points were then cross-
162 correlated between the dated and undated profiles as described by Adams et al. (2018).

163

164 3.3. *n*-alkanes: extraction, fractionation, instrumental analyses and quality assurances

165 The analytical method for hydrocarbons was described in detail by Wisnieski et al. (2016).
166 Approximately 10 g of sediments were Soxhlet extracted for 8 hours with 80 mL of a mixture of
167 dichloromethane (DCM) and *n*-hexane (1:1, v:v) and 100 µL of a surrogate standard mixture
168 containing 1-hexadecene and 1-eicosene (50 ng µL⁻¹) was added to each sample and blanks prior
169 extraction. This organic extract was reduced to *ca.* 2 mL by rotoevaporation, purified and
170 fractionated using 3.2 g of silica (silica gel 60, 0.063 – 0.200 mm; 5% deactivated with Milli-Q®
171 water) and 1.8 g of alumina (aluminium oxide 90 active, 0.063 – 0.200 mm; 5% deactivated with
172 Milli-Q® water) column chromatography. The samples were eluted with 10 mL of *n*-hexane to
173 obtain the aliphatic hydrocarbon fraction, containing *n*-alkanes and the isoprenoids pristane and
174 phytane. Sample extracts were concentrated to 500 µL and 100 µL of the internal standard 1-
175 tetradecene solution (50 ng µL⁻¹) was added prior to instrumental analysis.

176 The hydrocarbons were determined by the injection of 2 µL of the extract into a gas
177 chromatograph Agilent GC (model 7890A) equipped with a flame ionization detector and an
178 Agilent 19091J-413 capillary fused silica column coated with 5% diphenyl/dimethylsiloxane (30

179 m length, 0.32 mm ID, and 0.25 μm film thickness). Hydrogen was used as the carrier gas. The
180 injector and detector temperatures were adjusted to 280 $^{\circ}\text{C}$ and 325 $^{\circ}\text{C}$, respectively. Splitless
181 injection mode was adopted. The following oven temperature program was employed for analyses:
182 40–60 $^{\circ}\text{C}$ at 20 $^{\circ}\text{C min}^{-1}$, 60 $^{\circ}\text{C}$ for 2 min, 60–290 $^{\circ}\text{C}$ at 5 $^{\circ}\text{C min}^{-1}$, 290 $^{\circ}\text{C}$ for 5 min, 290–300 $^{\circ}\text{C}$
183 at 5 $^{\circ}\text{C min}^{-1}$, and 300 $^{\circ}\text{C}$ for 9 min. The individual compounds were identified by matching their
184 retention times with those obtained for external standard mixture (*n*-C₁₀ to *n*-C₄₀, pristane and
185 phytane) and quantified using a calibration curve ranging from 0.25 to 10.0 ng μL^{-1} . The detection
186 limits (DL) were 0.01 $\mu\text{g g}^{-1}$ for individual compounds. These data are based on the lowest
187 instrumental sensitivity of *n*-alkanes concentration (0.02 ng μL^{-1} , respectively) multiplied by the
188 final extracted volume (500 μL) and divided by the sediment weight (10 g) before extraction.

189 The procedural blanks showed that no peaks interfered with the analyses of the target
190 compounds. Mean recoveries of the surrogate standards, 1-hexadecene and 1-eicosene, ranged
191 from 50 to 99 % (mean = 66 ± 10 , N = 61) and from 56 to 106 % (mean = 78 ± 12 , N = 63), for at
192 least 90 and 93 % of samples analyzed, respectively. The precision, expressed as the coefficient
193 of variation between triplicates of the standard reference material (SRM) provided by International
194 Atomic Energy Agency (IAEA-408) was lower than 15 % for at least 85 % of compounds
195 analyzed. The measured concentrations of target parameters available in the IAEA-408 reference
196 sheet (e.g., total *n*-alkanes, *n*-C₁₇, *n*-C₁₈, pristane and phytane) in the SRM were in good agreement
197 with the certified values (lower than 15 %).

198

199 3.4. Data analysis

200 To explore temporal trends in the individual odd *n*-alkanes data (*n*-C₁₅ to *n*-C₃₅), a
201 constrained hierarchical cluster analysis was applied to a Euclidian distance of normalized values,
202 i.e., based on each individual *n*-alkane concentration divided by the sum of odd total *n*-alkanes (*n*-
203 C₁₅ to *n*-C₃₅). The clustering of the individual odd *n*-alkane (*n*-C₁₅ to *n*-C₃₅) data were used to

204 visualize stepwise changes in the *n*-alkane contributions along the cores. The clustered core
205 sections appear to represent environmental changes reflected by different *n*-alkane distributions
206 and were therefore used as ‘zones’ to be evaluated in detail in each sediment core. These zones
207 could be representative of different predominance of *n*-alkanes, and consequently, sources of
208 sedimentary OM. Broken stick analysis was performed to visualize the residual dispersion of the
209 hierarchical classification, and to determine the number of significant zones within the
210 sedimentary *n*-alkanes profile. The constrained hierarchical cluster and broken stick analysis were
211 performed in R using the *rioja* package (Juggins, 2020)

212 Principal Component Analysis (PCA) was also adopted as a multivariate approach to verify
213 which individual odd *n*-alkanes (*n*-C₁₅ to *n*-C₃₅) may best explain the core sections through each
214 core, thereby helping to identify the main sources of OM and their possible variations over the
215 period. PCA was performed using these same normalized data sets (individual *n*-alkanes) in order
216 to indicate which variable(s) may explain the zones formed in the cluster analyses. The PCA was
217 applied and plotted using R and the packages *factoMineR* and *factextra*, respectively (Husson et
218 al., 2016).

219 Box- and whisker plots were constructed to display the trends of *n*-alkanes and ratios across
220 depth zones for each sediment core, with median, first and third quartile, outlier and extreme values
221 indicated. Box-plots were created in the Statistica TIBCO® Software (v.14.0.0).

222

223 3.5. Diagnostic ratios for OM source identification and depositional conditions

224 The odd/even (O/E) ratios, carbon preference indices (CPI), terrestrial-to-aquatic ratios
225 (TAR), aquatic proxy ($P_{aq\ wax}$) and the metric average chain length (ACL) ratio were the *n*-alkane
226 proxies calculated in this study. The isoprenoids pristane and phytane were also included based on
227 their ratios with selected *n*-alkanes. Detailed information regarding equations, diagnostic values
228 and source assignment are presented in Table 1 and as Supplementary Information (Sections 1 and
229 2).

230 4. Results and Discussion

231 4.1. Core chronologies

232 The radiometric dating and loss-on-ignition profiles for both SLNG04C and BRYT02C
233 cores are shown in Supplementary Information (Fig. S1 and S2). The LOI₅₅₀ profiles for the
234 sediment cores 'B' and 'C' from each lake show good agreement (Fig. S1 and S2) and were used
235 to apply dates to undated SLNG04B and BRYT02B cores (Adams et al., 2018). The cross-
236 correlation of LOI₅₅₀ records from cores SLNG04C and BRYT02C with those from SLNG04B
237 and BRYT02B allow chronologies to be allocated extending to *ca.* 1835 (179 years) and *ca.* 1915
238 (99 years), respectively.

239

240 4.2. The *n*-alkane levels and distributions in the studied shallow lakes

241 Tables S1–S2 display the *n*-alkanes and isoprenoids concentrations. The sum of individual
242 *n*-alkanes from *n*-C₁₄ to *n*-C₃₅ (Total *n*-Alk (C₁₄-C₃₅)) concentrations ranged from 2.02 to 61.5 μg
243 g⁻¹ (median = 28.2 ± 12.0) in SLNG04B and from 35.9 to 106.9 μg g⁻¹ (median = 60.1 ± 13.8) in
244 BRYT02B (Fig. S3). These levels are considered high when compared to sediments from a
245 paleothermocarst lake on the Bykovsky Peninsula, northeastern Siberia (0.6 - 20.8 μg g⁻¹;
246 Jongejans et al., 2020) and surficial sediments from Lake Baikal collected in summer 2001 (4 - 55
247 μg g⁻¹; Russell and Rosell-Melé, 2005).

248 In general, the analyzed samples for both cores presented significant levels of long-chain
249 *n*-alkanes (LC *n*-Alk; *n*-C₂₇ to *n*-C₃₂) followed by mid-chain (MC *n*-Alk; *n*-C₂₁ to *n*-C₂₆) and short-
250 chain *n*-alkanes (SC *n*-Alk; *n*-C₁₅ to *n*-C₂₀) (Tables S1 and S2; Fig. S3). The contribution of the
251 SC *n*-Alk in the Total *n*-Alk is low in the lower core sections, likely due to high lability of the low
252 molecular weight hydrocarbons. A unimodal distribution of *n*-alkanes is observed in all samples
253 analyzed, reaching a maximum between *n*-C₂₇ to *n*-C₃₃. The *n*-C₂₉ was the predominant *n*-alkane
254 in SLNG04B, while *n*-C₂₇ was dominant in BRYT02B (Fig. S4). This *n*-alkane distribution is

255 typical for Holocene age sediment in both Lake Baikal (Brincat et al., 2000; Russell and Rosell-
256 Melé, 2005) and in Lake Billyakh, northern Siberia (Tarasov et al., 2013).

257
258 *4.3. Changes in the sedimentary OM composition and ecological structure based on n-alkane and*
259 *isoprenoids proxies in the studied shallow lakes*

260 *4.3.1. The SLNG04 lake*

261 The SLNG04B record can be divided in 4 zones from the bottom to the top (Fig. 4) based
262 on cluster and broken stick analyses (Fig. S5 and S6). These four distinct zones correspond to
263 variations in the PCA scores (Fig. S7) and along depth (Fig. S8).

264
265 • Zone 1 (*ca.* 1835 to *ca.* 1875; 63 – 50 cm)

266 Zone 1 is primarily influenced by grasses/herbs (high relative percentages of $n\text{-C}_{31}$, $n\text{-C}_{33}$
267 and $n\text{-C}_{35}$; Fig. S9) and non-emergent vascular plants ($n\text{-C}_{25}$ and $n\text{-C}_{27}$; Fig. S9). Zone 1 presented
268 relatively low concentrations of all groups of n -alkanes (SC, MC and LC n -Alk), reflective in the
269 low values of Total n -Alk (Fig. 3). This is consistent with relatively low levels of LOI₅₅₀ at this
270 time. The combined Total n -Alk and LOI₅₅₀ records during the early- to mid-19th century may
271 indicate a time during lake development, progressing from a marginal semi-aquatic or terrestrial
272 site to a lake basin. In fact, the main distinction between this stage and the rest of the core is related
273 to the major influence of $n\text{-C}_{25}$ and $n\text{-C}_{27}$, related to non-emergent vascular plants, typically found
274 in a semi-terrestrial or marshy ecosystem transition (Luoto et al., 2017), also corroborated by P_{aq}
275 _{wax} values (< 0.35) (Fig. 5) associated with a mixed source. This particular individual n -alkanes
276 contribution is reflected in the lower values of ACL found in Zone 1 (Fig. 5). Low concentrations
277 of SC and MC n -Alk in Zone 1 indicate a low contribution from autochthonous OM sources (Fig.
278 3). The absence of submerged aquatic macrophytes and aquatic animal remains, an absence of

279 preserved algal pigments, and very low diatom concentrations were also verified in this part of the
280 core (Adams, 2017), and are consistent with the individual *n*-alkanes distribution.

281 The low preservation of OM in the Zone 1 is corroborated by the relatively low values of
282 O/E and CPI diagnostic ratios in this stage (outliers to CPI₁, Fig. S10 and S11), and the high values
283 to TAR (outliers, Fig. S12) compared to middle and top core sections (Fig. 5). The higher exposure
284 to light and air at SLNG04 lake prior to the mid-19th century increased the degradation of labile
285 components of sedimentary OM (Reuss et al., 2005), and consequently, isoprenoids (pristane and
286 phytane) (Fig. 6) and pigments (Adams, 2017). Low levels of preserved OM content and low *n*-
287 alkanes concentrations may be tied to depositional oxic conditions, as indicated by the maximum
288 Fe/Mn and minimum Ca/Ti ratios that occurred in this period (Adams, 2017). On the other hand,
289 the LC *n*-Alk that are more resistant to degradation were also present in relatively low
290 concentrations, and may be related to low values of LOI₅₅₀ in the bottom of the core.

291

292 • Zone 2 (*ca.* 1880 to *ca.* 1910; 47 – 38 cm)

293 Zone 2 is influenced by grasses/herbs and higher plants (Fig. S9). Both Zones 1 and 2 are
294 under strong influence of terrestrial sources of organic matter. Low concentrations of SC and MC
295 *n*-Alk concentrations suggests the low contribution of aquatic sources; however, this may also be
296 due to higher degradation rates of these compounds.

297 Zone 2 presented a slight increase in concentrations of LC *n*-Alk (and consequently in Total
298 *n*-Alk) compared to the Zone 1 (Fig. 3); it was consistent with the increase of LOI₅₅₀ values found
299 in this section of the core, which reached the maximum OM content of the core at 38 cm (*ca.*
300 1910).

301 The main distinction between this zone and the rest of the core is related to the major
302 influence of *n*-C₃₁, *n*-C₃₃ and *n*-C₃₅ in the Total *n*-Alk concentration, that are related to grasses and
303 herbs (Fig. S9). This contribution is well marked due the higher ACL values (outliers, Fig. S12)

304 found in Zone 2. The environmental changes in Zone 2, indicated by the *n*-alkanes and related
305 diagnostic ratios (TAR and ACL; Fig. 5), reflected changes in the allochthonous OM input. The
306 deposition of allochthonous OM from vascular plants, grasses and herbs in the Selenga Delta
307 created a deeper open water zone, now hospitable to diverse communities of submerged and
308 floating macrophytes. The low preservation of OM observed during Zone 1 continued into Zone
309 2, indicated by the relatively low values of O/E and CPI diagnostic ratios in this stage (Fig. 5).

310 The low levels of *n*-C₁₇ and *n*-C₁₉, primarily related to phytoplankton, is consistent with
311 the absence of preserved diatoms frustules during this period (Adams, 2017). Shallow depths at
312 this time potentially led to increased turbulence, increased mixing, and increased wave-action, and
313 consequently, the degradation of sedimentary OM. Biological parameters reinforced the
314 environmental changes in Zone 2 due to the slight increase in diatom concentrations, consisting
315 mainly of epiphytic and small benthic diatoms (Adams, 2017). These geochemical and biological
316 features suggest the transition period to the permanent inundation of Selenga Delta (Gell et al.,
317 2007), characterized by a small, shallow-water, high-closure system with mostly littoral and
318 epiphytic habitats (Hay et al., 2000; Summers et al., 2017).

319

320 • Zone 3 (ca. 1915 to ca. 1945; 35 – 25 cm)

321 Zone 3 marks a transition on the main components of sedimentary OM, from non-emergent
322 vascular plants (*n*-C₂₅ and *n*-C₂₇) and grasses/herbs (*n*-C₃₁, *n*-C₃₃) to submerged and floating
323 macrophytes (*n*-C₂₃ and *n*-C₂₅) and phytoplankton (*n*-C₁₇, *n*-C₁₉) (Fig. S9). This is primarily shown
324 by the increase of P_{aq wax} index and, also by a decrease in TAR values (Fig. 5). In addition, the
325 CPI₂ values are typical of terrestrial sources associated with higher plants (*n*-C₂₉), that are an
326 important OM source throughout the core (Fig. 5).

327 Zone 3 showed a clear increase in concentrations of different groups of *n*-alkanes compared
328 to the previous zones and is consistent with the concurrent variation in LOI₅₅₀ (Fig. 3). Similar

329 concentrations of SC and LC *n*-Alk compared to Zone 2 were detected. An increase in MC *n*-Alk
330 was noted in the lower sections of this zone (*ca.* 1915 to *ca.* 1925; 35 – 32 cm), while a fast and
331 prominent increase in *n*-alkane concentrations in the upper sections occurred (*ca.* 1925 to *ca.* 1945;
332 32 – 25 cm) (Fig. 3). The decrease in ACL in this zone may represent an increase in sedimentary
333 *n*-C₂₉ as a consequence of deforestation (Meyers, 2003; Aichner et al., 2010).

334 There was an increase in the preservation of OM in Zone 3, indicated by increased values
335 of O/E and CPI diagnostic ratios compared to previous zones (Fig. 5). This zone contained the first
336 detectable levels of isoprenoids. Higher values of Pri/Phy, Pri/*n*-C₁₇ and Phy/*n*-C₁₈ ratios were
337 obtained compared to the rest of the core (Fig. 6 and S13) suggesting an increase in anoxic
338 conditions and corroborated by minimum Fe/Mn ratios *ca.* 1920 (Adams, 2017).

339

340 • Zone 4 (*ca.* 1945 to 2014; 25 – 0 cm)

341 Zone 4 showed the highest concentrations of different groups of *n*-alkanes and LOI₅₅₀ (Fig.
342 3). Fresh aquatic OM from phytoplankton (*n*-C₁₇ and *n*-C₁₉) and submerged and floating
343 macrophytes (*n*-C₂₁ and *n*-C₂₃) play an important role in the sedimentary OM in this most recent
344 zone. Notably, we observed an increase followed by a slight decrease in Total *n*-Alk concentration
345 and LOI₅₅₀ between *ca.* 1945 to *ca.* 1980 (25 – 11.5 cm) (Fig. 3), after which levels remained
346 slightly higher through to the top of the core.

347 Highest levels of Total *n*-Alk, particularly SC and MC *n*-Alk, are expected to be found in
348 the more surficial sections of sediment cores due the recent input of fresh autochthonous OM
349 (Hedges et al., 1997). Also, the individual *n*-alkanes distribution within the PCA confirmed the
350 establishment of current connectivity and sedimentary environmental, with a greater contribution
351 of autochthonous OM from submerged and floating macrophytes (*n*-C₂₃ and *n*-C₂₅) and
352 phytoplankton (*n*-C₁₇, *n*-C₁₉). This is also evidenced by the lowest TAR values of the entire core
353 and the constant P_{aq wax} values (Fig. 5). However, the main contribution continued to be from

354 higher plants ($n\text{-C}_{29}$) due to the connection to the Selenga River, and the influx of river-derived
355 terrestrial matter. The slightly higher values of ACL, when compared to Zone 3, confirm this (Fig.
356 5).

357 Trends in total $n\text{-Alk}$ are consistent with biological parameters that indicate maximum lake
358 productivity levels in the late-1950s, notably pigment concentrations in the SLNG04 lake (Adams,
359 2017). Increasing SC $n\text{-Alk}$ up to *ca.* 1965, are in agreement with greater diatom concentrations
360 at *ca.* 1960 (Adams, 2017) as phytoplankton are an important source of $n\text{-C}_{17}$ and $n\text{-C}_{19}$. Changes
361 in macrophyte assemblages can influence changes in other biological communities, including
362 diatoms (Sokal et al., 2010), and may be reflected in the distribution of individual $n\text{-alkanes}$, and
363 related indices such as O/E ($< \text{C}_{24}$), CPI₁ and P_{aq wax} (Fig. 5).

364 Changes in delta morphology in the late-20th and early-21st centuries caused a shift in
365 discharge from the southwestern to the northeastern branches of the Selenga River Delta (Chalov
366 et al., 2016), with severe implications for sediment and chemical transport and river water flow.
367 Connectivity to the river dictated the abundance and diversity of the diatoms present (as indicated
368 by the high contribution of SC $n\text{-Alk}$ to the sediment) with a higher diversity reflecting higher
369 connectivity sites and the presence of planktonic species in lakes connected to the Selenga River.
370 Therefore, it is also possible that decreased macrophyte biomass (indicated by low contribution
371 of MC $n\text{-Alk}$) at high connectivity sites is related to increased connectivity with the Selenga River.

372 The regular and relatively high values of O/E and CPI found in this zone are related to fresh
373 and/or preserved OM, and despite the recent increase in human activities in the Selenga River
374 basin, the hydrocarbons found may be primarily related to biogenic sources. The isoprenoids ratios
375 (Pri/Phy, Pri/ $n\text{-C}_{17}$ and Phy/ $n\text{-C}_{18}$) showed decreasing values in this zone reaching a minimum at
376 the top core (Fig. 6) and reflecting the evolution of anoxic conditions in this zone due to the large
377 amount of deposited OM.

378

379 4.3.2. *The Black Lake*

380 The BRYT02B record can be divided in 2 main zones (Fig. 4) based on cluster and broken
381 stick analyses (Fig. S14 and S15). The top core section (0 – 2 cm) was removed from these analyses
382 as it represented a single sample composed of high amounts of fresh OM and high SC *n*-Alk
383 concentrations. The two identified zones are distinguished by variations in PC1 scores (Fig. S7)
384 with depth (Fig. S16).

385

386 • Zone 1 (*ca.* 1915 to *ca.* 1980, 67.5 – 23 cm)

387 Zone 1 is primarily influenced by submerged and floating macrophytes (high/moderate
388 percentages of *n*-C₂₁ and, *n*-C₂₃, respectively), non-emergent vascular plants (high/moderate
389 percentages of *n*-C₂₅) and higher plants (high/moderate percentages of *n*-C₂₉, respectively) (Fig.
390 S17).

391 Vascular plants (*n*-C₂₉) and submerged and floating macrophytes (*n*-C₂₃ and *n*-C₂₅) were
392 the major components of sedimentary OM in mid- (*ca.* 1945 to *ca.* 1955; 50 – 40 cm) and lower
393 (*ca.* 1915 to *ca.* 1945; 67.5 – 50 cm) sections of this zone (Fig. S7 and S17), as confirmed by the
394 lower ACL, increasing P_{aq wax} index and decreasing TAR values in this part of the core (Fig. 5).
395 The upper sections of this zone (*ca.* 1955 to *ca.* 1980; 40 – 23 cm) may represent the transition
396 from an environment typically influenced by allochthonous sources (higher plants), with
397 grasses/herbs appearing as an important fraction of terrestrial OM input, to an increase in
398 sedimentary allochthonous OM from phytoplankton (*n*-C₁₅, *n*-C₁₇ and *n*-C₁₉) (Fig. S17), as verified
399 by inverse trends of P_{aq wax} index and TAR when compared with lower sections of this zone (Fig.
400 5).

401 Zone 1 showed a general decrease and slight fluctuation in the LOI₅₅₀ values and Total *n*-
402 Alk concentrations (Fig. 3), and contained mainly MC and LC *n*-Alk until *ca.* 1955, while SC *n*-
403 Alk concentration increased until *ca.* 1960. Between *ca.* 1955 and *ca.* 1980 the concentrations of

404 all classes of *n*-alkanes and LOI₅₅₀ values oscillated between their recorded maximum and
405 minimum values (Fig. 3). Magnetic susceptibility values were low and decreased through Zone 1,
406 with low fluctuations throughout this section of the core (Adams, 2017), suggesting decreased
407 input of terrestrial materials.

408 The values of O/E and CPI in this zone indicate preserved OM and the absence of
409 anthropogenic hydrocarbons, with a marked influence from terrestrial higher plants in the mid-
410 and bottom sections. A decrease in the O/E (< C₂₄) and CPI₁ ratios (both related to SC and MC *n*-
411 Alk) was observed in the upper sections (Fig. 5), which may indicate the presence of oil
412 hydrocarbons sources. Indeed, the input of hydrocarbons related to crude oil and by-products has
413 been previously characterized in Black Lake (Adams et al., 2018), by the increased concentrations
414 of low molecular weight polycyclic aromatic hydrocarbons (PAHs with 2-3 rings) after *ca.* 1970
415 and low values (< 0.10) of the anthracene / anthracene + phenanthrene (Ant/178) ratio after *ca.*
416 1960, that are typically associated with petroleum sources and its by-products (Yunker et al.,
417 2002).

418 The individual *n*-alkanes distribution and related ratios corroborate the pigment and diatom
419 records from the early-20th century, indicating low productivity, characterized primarily by low
420 algal concentrations and biomass (i.e., low relative contribution of SC *n*-Alk) (Adams, 2017).
421 Macrophyte communities in Black Lake in the early-1900 (Eftesum, 2017), showed the
422 predominance of *Chara* spp, a common species in lower productivity, clear-water shallow lakes,
423 with stable and diverse macrophyte communities (Bazarova and Itigilova, 2006; Sayer et al.,
424 2010). This autochthonous source of sedimentary OM is recorded by relatively high MC *n*-Alk
425 (i.e., *n*-C₂₃ and *n*-C₂₅) levels in this zone. Changes found in the biomarker analyses in the mid-20th
426 century (*ca.* 1960) also verified a shift in both pigment concentration and diatom assemblage
427 records at Black Lake (Adams, 2017).

428 The Pri/Phy ratio presented decreasing values ratios in this zone reaching the minimum
429 around *ca.* 1970, remains constant until the top core (Fig. 6), reflecting changes in the oxic (> 2)
430 to redox (< 1) environmental conditions. On the other hand, the Pri/*n*-C₁₇ and Phy/*n*-C₁₈ presented
431 low and relatively constant values in mid- and lower sections (until *ca.* 1955) (Fig. 6), related to
432 high water column productivity and preserved OM in the sediments. A slight increase and relative
433 steady values until top core on Pri/*n*-C₁₇ and Phy/*n*-C₁₈ suggest different relative biodegradation
434 rates of *n*-alkanes and the corresponding isoprenoids under anoxic conditions (as indicated by
435 Pri/Phy ratio) (Commendatore and Esteves, 2004). Total algal pigments (chlorophyll-*a* and
436 pheophytin-*a*) are precursors of isoprenoids and high levels were presented in the Black Lake
437 pigment record from *ca.* 1965 until the top core (Adams, 2017), explaining a marked contribution
438 of pristane and phytane in upper sections until recent years.

439

440 • Zone 2 (*ca.* 1980 to *ca.* 2010; 23 – 2 cm)

441 Zone 2 represented a stable period for the lake with an important contribution of fresh
442 aquatic OM from phytoplankton (high/moderate relative percentages of *n*-C₁₅ and *n*-C₁₉ and, *n*-
443 C₁₇) and terrestrial components associated with grasses/herbs (high/moderate relative percentages
444 of *n*-C₃₁, *n*-C₃₃ and *n*-C₃₅) (Fig. S17), especially between *ca.* 1985 and *ca.* 1995.

445 Zone 2 showed lower concentrations of MC and LC *n*-Alk compared to the previous zone,
446 while SC *n*-Alk concentrations remained constant to the top of the core (Fig. 3). A slight decrease
447 in Total *n*-Alk concentrations was observed while LOI₅₅₀ values were relatively stable (Fig. 3).
448 The individual *n*-alkanes distribution, based on the PCA, confirm the establishment of a new
449 sedimentary environment with a significant autochthonous OM contribution as indicated by *n*-
450 alkanes from phytoplankton (*n*-C₁₅, *n*-C₁₇, and *n*-C₁₉) and more input from grasses/herbs (*n*-C₃₁
451 and *n*-C₃₃) together with vascular plants (*n*-C₂₉) from allochthonous sources. Lower TAR and
452 steady P_{aq wax} values suggest ‘fresher’ OM from autochthonous sources from *ca.* 1980 (Fig. 5).

453 The values of O/E and CPI ratio oscillated in Zone 2, and are typical of fresh OM with a
454 marked influence from terrestrial sources and higher plants (as suggested by O/E ($> C_{23}$) and CPI
455 ₂ ratios that are related to more refractory compounds). However, decreasing O/E ($< C_{24}$) and CPI₁
456 ratios from *ca.*1980 to *ca.* 2004 may be associated with oil hydrocarbon sources, towards the end
457 of Zone 1. Relatively anoxic conditions (as indicated by Pri/Phy < 0.5) may prevent extensive
458 degradation of fresh OM; so, the lower values of these ratios may not be associated to the
459 degradation of *n*-alkanes.

460 The increases in abundances of several planktonic diatom species from *ca.* 1960, and more
461 intensively *ca.* 1980 (represented by SC *n*-Alk in the PCA, Fig. S13) may be attributed to increases
462 in nutrient-associated levels of turbidity, declines in light penetration, and declines in submerged
463 macrophyte abundances (represented by low significance of *n*-C₂₃ and *n*-C₂₅) in Zone 2 (Fig. S17)
464 (Adams, 2017). Increases in the proportion of planktonic species, also indicated by increasing
465 pigment and isoprenoids concentrations, suggest increasing eutrophication and a shift towards
466 pelagic-dominated primary production (Battarbee et al., 2001; Sayer et al., 2010).

467

468 *4.4. Depositional history at the Selenga River basin*

469 SLNG04 and Black Lake have undergone several major shifts in state, structure, and likely
470 functioning since the early-19th century reflecting environmental changes in the Selenga River
471 basin. Biomarkers concur with palaeolimnological records and revealed that changes in
472 sedimentary OM at the mid/end-19th century in the Selenga Delta coincide with the Tsagan
473 earthquake just off-shore of the Delta in 1862. The earthquake was the strongest ever recorded in
474 east Siberia (with a magnitude of 7.5) and was integral in forming the contemporary structure of
475 the right bank of the Selenga Delta (Vologina et al., 2010). This seismic event resulted in
476 substantial subsidence and flooding of a large area of the northeast corner of the Delta, with a total
477 area of approximately 200 km² (Orlov, 1872). Furthermore, a catastrophic flood event in the late-

478 19th century in Transbaikalia, flooding many towns and villages along the Selenga River, caused
479 an increase in the river height by 4 metres within one day (Kadetova and Radziminovich 2014),
480 was likely responsible for increased input of allochthonous OM, trace and major elements in the
481 Selenga Delta at this time (Yang et al., 2016). The apparent predominance of allochthonous
482 sources from vascular plants, grasses and herbs buried in the SLNG04 lake seems be related to the
483 Tsagan earthquake and the transport of these materials from the drainage basin to the Delta due
484 extreme flooding events. Also, the Tsagan earthquake of 1862 and the flood event in the late-19th
485 century contributed to high sediment exposure to light and air increasing the degradation of labile
486 components of sedimentary OM and increasing the oxic potential of the sediments at this time,
487 due to high levels of sediment influx/erosion to the site (Gell et al., 2007) during this period
488 (Adams, 2017).

489 Land-use conversion for agricultural expansion and intensification began in the Selenga
490 River basin in the early-19th century as a response to increased populations in the region due the
491 development of the Trans-Siberian Railroad and mining operations in different portions of this
492 area (Robinson and Anisova, 2004). Agricultural expansion was the primary cause of massive
493 deforestation events and land conversion from boreal forest-steppe (higher plants, with
494 predominance of *n*-C₂₉) to croplands in the 19th century in the Selenga Delta and Lake Gusinoye
495 regions. These land conversions resulted in an increase in the erosion and transport of sediment
496 and allochthonous OM directly into the Selenga River affecting large areas of the basin (Eimers et
497 al., 2008; Bazhenova and Kobylkin, 2013). Also, increased agriculture within the Selenga River
498 basin during this period resulted in increasing eutrophic conditions that was reflected in changes
499 in the main components of sedimentary OM, from non-emergent vascular plants and grasses/herbs
500 to submerged and floating macrophytes and phytoplankton in Selenga Delta (Fig. S9).

501 Further agricultural expansion in the Selenga River basin occurred intensively from the
502 mid-1950s, with a peak around the 1980s (Robinson and Anisova, 2004), and contributed to an

503 increase to hypereutrophic conditions in the Selenga Delta, and increasing the contribution of
504 autochthonous OM to the sediments (Fig. 3). Increased connectivity to the Selenga River,
505 increased agricultural activity and anthropogenic disturbances within the Selenga River basin in
506 the early-20th century likely resulted in increased nutrient flux to the Selenga Delta. A possible
507 mechanism relates to stimulated plant production (submerged and floating macrophytes), leading
508 to increased photosynthetic removal of CO₂ from the water column, resulting in increasing pH
509 (Potasznik and Szymczyk, 2015). A higher pH would lead to increased phosphorus release from
510 sediments (Koski-Vahala et al., 2001; Wu et al., 2014), thereby stimulating plant productivity
511 during the early- to mid-20th century, as well as slight reducing conditions in the Selenga Delta.

512 Population growth after the end of World War II, as well as intensive increases in livestock
513 populations until *ca.* 1990, contributed to the increase in nutrient flux to soils, and increased
514 sediment erosion within the Selenga River basin (Bazhenova and Kobylkin, 2013). The enrichment
515 from increased populations and intensification of agricultural practices drove the observed changes
516 found in the sedimentary OM in the mid-20th century (*ca.* 1960) at Black Lake. Differing controls
517 for OM and mineral supply has been assumed in Lake Gusinoye region post-1950 (Adams, 2017),
518 indicating a higher influx of mineral sources and coinciding with increased development and
519 industrialization near Lake Gusinoye in the 1950s (Pisarsky et al., 2005).

520 The construction of the Irkutsk Hydroelectric Dam along the Angara River (the only
521 outflow from Lake Baikal) was completed in the mid-1950s. The filling of the associated reservoir
522 was completed in 1963 and the environments surrounding of the Lake Baikal, and were submerged
523 (Pinegin et al., 1976), increasing the water depth, surficial area and the connectivity of Selenga
524 Delta with Selenga River, promoting changes in submerged macrophyte and diatom communities
525 (Brock et al., 2011). These features may have contributed to increased preservation of sedimentary
526 OM and substantial changes in sedimentary redox conditions since *ca.* 1940 and, as well as to the
527 development of diatom assemblages in the early-1960s (Adams, 2017). Indeed, the sharp, though

528 temporary, increase in sedimentation rate in the early-1960s (1963 ± 4 yrs) may correspond with
529 the timing of the flood associated with the construction of the Irkutsk Dam and may contribute to
530 the evolution of anoxic conditions and preservation of a large amount of deposited OM.

531 The decades after the end of World War II were characterized by intense economic growth
532 and industrial expansion in the USSR, and industrial and mining growth in the Lake Gusinoye
533 region (Pisarsky et al., 2005). This may have increased petroleum product demand (e.g., diesel
534 fuel, motor oil), increasing usage and consequently, indirect input to the environment and the
535 occurrence of oil hydrocarbons in aquatic systems as indicated by *n*-alkanes and polycyclic
536 aromatic hydrocarbons in sediments of the region (Adams et al., 2018).

537

538 **5. Conclusions**

539 The drivers of sedimentary OM composition and sources since the 19th century in the
540 Selenga River basin have been both natural and anthropogenically-induced. Local natural
541 disturbances, regional natural variability in climate, and anthropogenic stressors have resulted in
542 ecological responses within the Selenga River basin during the last two centuries, including the
543 composition of lacustrine sedimentary OM.

544 The greatest period of agricultural expansion (resulting in wide-scale deforestation) and
545 population growth in the Selenga River basin occurred in the mid-20th century, and was closely
546 linked with periods of economic development in Russia. Changes in hydrological regimes (flood
547 events), and nutrient pollution, changed the composition of sedimentary OM in the region.

548 The SLNG04B record extends back to the early-19th century, while the record from Black
549 Lake extends only to the late-19th century. Within the period covered by these records, the primary
550 finding is the biomarker response to the elevated nutrient levels related to increasing regional
551 anthropogenic development in southeast Siberia, with agricultural intensification in the early-20th

552 century, and economic and industrial intensification following World War II in the early to mid-
553 20th century.

554 The individual *n*-alkanes and their related proxies provide valuable information on the
555 origin, degradation level and deposition conditions of the deposited OM over the last two centuries
556 in southern Siberia and can be used to corroborate ecological changes in freshwater floodplain
557 wetlands.

558

559 **Acknowledgments**

560 We wish to acknowledge the various agencies who helped to fund this work, especially CAPES
561 (Coordenação de Aperfeiçoamento de Pessoal de Ensino Superior) in the ambit of PRINT project
562 by financial support (88887.311742/2018-00 and 88887.477472/2020-00) to CCM, a UCL
563 Graduate School Research grant to JKA, UK NERC (NE/J010227/1) to AWM, RFBR grant N°
564 16-05-00586, Integration Project SB RAS N° 0341-2016-001, project N° 0346-2016-0005 and
565 RSF grant N° 16-17-10079 (field work, coring and geomorphology) to AAS. The authors wish to
566 thank D. White for assistance during field collection of the sediment cores, and J. da Silva and
567 A.C. Souza for support during the laboratory procedures and instrumental analysis of organic
568 markers. This work as part of the activities established in the Memorandum of Understanding on
569 Environmental Change research between UCL (UK) and UFPR (Brazil).

570

571 **References**

572 Aboul-Kassim, T.A.T., Simoneit, B.R.T., 1996. Lipid geochemistry of surficial sediments from
573 the coastal environment of Egypt I. Aliphatic hydrocarbons – characterization and sources.
574 Mar. Chem. 54, 135–158.

575

576 Adams, J.K., 2017. Multiproxy reconstructions of recent environmental change: understanding the
577 ecological response of shallow lakes within the Selenga River Basin, Southeast Siberia, to
578 anthropogenic and natural disturbances. Unpublished PhD thesis. Department of
579 Geography, University College London.

580 Adams, J.K., Martins, C.C., Rose, N.L., Shchetnikov, A.A., Mackay, A.W., 2018. Lake sediment
581 records of persistent organic pollutants and polycyclic aromatic hydrocarbons in southern
582 Siberia mirror the changing fortunes of the Russian economy over the past 70 years.
583 Environ. Pollut. 242, 528–538.

584 Aichner, B., Herzsuh, U., Wilkes, H., Vieth, A., and Böhner, J. 2010. δ D values of *n*-alkanes
585 in Tibetan Lake sediments and aquatic macrophytes – A surface sediment study and
586 application to a 16-ka record from Lake Koucha, Org. Geochem. 41, 779–790.

587 Appleby P.G., Oldfield, F., 1978. The calculation of ^{210}Pb dates assuming a constant rate of supply
588 of unsupported ^{210}Pb to the sediment. Catena 5, 1–8.

589 Appleby, P.G., 2001. Chronostratigraphic techniques in recent sediments. In: Tracking
590 Environmental Change Using Lake Sediments. Vol. 1: Basin Analysis, Coring, and
591 Chronological Techniques. Kluwer Academic Publishers, The Netherlands.

592 Appleby, P.G., Nolan, P.J., Gifford, D.W., Godfrey, M.J., Oldfield, F., Anderson, N.J., Battarbee,
593 R.W., 1986. ^{210}Pb dating by low background gamma counting. Hydrobiologia 141, 21-27.

594 Battarbee, R.W., Jones, V., Flower, R., Cameron, N., Bennion, H., Carvalho, L., Juggins, S., 2001.
595 Diatoms. In Terrestrial, algal and siliceous indicators. Eds. J. Smol, H.J.B. Birks, and M.
596 Last, Kluwer Academic Publishers, The Netherlands. pp. 155–202.

597 Bazarova, B., Itigilova, M., 2006. Long-term production dynamics of aquatic vegetation in the
598 Arakhlei Lake (Eastern Transbaikalia). Biol. Bull. Russ. Acad. Sci. 33, 68–75.

599 Bazhenova, O.I., Kobylkin D.V., 2013. The dynamics of soil degradation processes within the
600 Selenga Basin at the agricultural period. Geogr. Nat. Resour. 34, 221–227.

601 Bourbonniere, R.A., Meyers, P.A., 1996. Anthropogenic influences on hydrocarbon contents of
602 sediments deposited in eastern Lake Ontario since 1800. *Environ. Geol.* 28, 22–28.

603 Bray, E.E., Evans, E.D., 1961. Distribution of *n*-paraffins as a clue to recognition of source beds.
604 *Geochim. Cosmochim. Acta* 22, 2–15.

605 Brincat, D., Yamada, K., Ishiwatayi, R., Uemura, H., Naraoka, H., 2000. Molecular-isotopic
606 stratigraphy of long-chain *n*-alkanes in Lake Baikal Holocene and glacial age sediments.
607 *Org Geochem.* 31, 287–294.

608 Brock, B.E., Martin, M.E., Mongeon, C.L., Sokal, M.A., Wesche, S.D., Armitage, D., Wolfe, B.B.,
609 Hall, R.I., Edwards, T.W.D., 2011. Flood frequency variability during the past 80 years in
610 the Slave River Delta, NWT, as determined from multi-proxy palaeolimnological analysis.
611 *Can. Water Resour. J.* 35, 281–300.

612 Chalov S., Romanchenko A.O., 2016. Linking catchments to rivers: Flood-driven sediment and
613 contaminant loads in the Selenga River. *Water and Environment in the Selenga-Baikal*
614 *Basin.* Karthe D., Chalov S., Kasimov H., & Kappas M (eds.) ibidem Press, Stuttgart, pp.
615 83–101.

616 Chalov, S., Thorslund, J., Kasimov, N., Aybullaatov, D., Ilyicheva, E., Karthe, D., Kositsky, A.,
617 Lychagin, M., Nittrouer, J., Pavlov, M., Pietron, J., Shinkareva, G., Tarasov, M., Garmaev,
618 E., Akhtman, Y., Jarsjo, J., 2016. The Selenga River delta: a geochemical barrier protecting
619 Lake Baikal waters. *Reg. Environ. Change* 17, 2039–2053.

620 Chen, F., Fang, N., Shi, Z., 2016. Using biomarkers as fingerprint properties to identify sediment
621 sources in a small catchment. *Sci. Total Environ.* 557-558, 123–133.

622 Chevalier, N., Savoye, N., Dubois, S., Lama, M.L., David, V., Lecroart, P., Menach, K.L.,
623 Budzinski, H.J., 2015. Precise indices based on *n*-alkane distribution for quantifying
624 sources of sedimentary organic matter in coastal systems. *Org. Geochem.* 88, 69–77.

625 Cobbaert, D., Wong, A., Bayley, S.E., 2014 Precipitation-induced alternative regime switches in
626 shallow lakes of the Boreal Plains (Alberta, Canada). *Ecosystems*, 17, 535–549

627 Commendatore, M.G., Esteves, J.L., 2004. Natural and anthropogenic hydrocarbons in sediments
628 from the Chubut River (Patagonia, Argentina). *Mar. Pollut. Bull.* 48, 910–918.

629 Davidson, N.C., Fluet-Chouinard, E., Finlayson, C.M., 2018. Global extent and distribution of
630 wetlands: Trends and issues. *Mar. Freshw. Res.* 69, 620–627.

631 Derrien, M., Yang, L., Hur, J., 2017. Lipid biomarkers and spectroscopic indices for identifying
632 organic matter sources in aquatic environments: a review. *Water Res.* 112, 58–71.

633 Didyk, B.M., Simoneit, B.R.T., Brassell, S.C., Eglinton, G., 1978. Organic geochemical indicators
634 of palaeoenvironmental conditions of sedimentation. *Nature* 272, 216–222.

635 Eftesum, E., 2017. Reconstructing shallow lake ecosystem dynamics in southeastern Siberia using
636 macrofossil analysis. Unpublished MSc thesis, Department of Geography, University
637 College London.

638 Eglinton, G., Hamilton, R.J., 1967. Leaf epicuticular waxes. *Science* 156, 1322–1335.

639 Eimers, M.C., Watmough, S.A., Buttle, J.M., Dillon, P.J., 2008. Examination of the potential
640 relationship between droughts, sulphate, and dissolved organic carbon at a wetland-
641 draining stream. *Glob. Chang. Biol.* 14, 938–948.

642 Ficken, K.J., Li, B., Swain, D.L., Eglinton, G., 2000. An n-alkane proxy for the sedimentary input
643 of submerged/floating freshwater aquatic macrophytes. *Org. Geochem.* 31, 745–749.

644 Freeman, K.H., Pancost, R.D., 2013. Biomarkers for terrestrial plants and climate. In *Treatise on*
645 *Geochemistry: 2nd Edition, Vol. 12*, pp. 395–416. JAI-Elsevier Science Inc.

646 Gell, P., Tibby, J., Little, F., Baldwin, D., Hancock, G., 2007. The impact of regulation and
647 salinization on floodplain lakes: the lower River Murray, Australia. *Hydrobiologia* 591,
648 135–146.

649 Hay, M.B., Michelutti, N., Smol, J.P., 2000. Ecological patterns of diatom assemblages from
650 Mackenzie Delta lakes, Northwest Territories, Canada. *Canad. J. Bot.* 78, 19-33.

651 Hedges, J.I., Keil, R.G., Benner, R. 1997. What happens to terrestrial organic matter in the ocean?
652 *Org Geochem* 27, 195–212.

653 Heiri, O., Lotter, A.F., Lemcke, G., 2001. Loss on ignition as a method for estimating organic and
654 carbonate content in sediments: reproducibility and comparability of results. *J. Paleolimnol.*
655 25, 101–110.

656 Hobbs, W.O., Lafrancois B.M., Stottlenyer, R., Toczydlowski, D., Engstrom, D.R., Edlund, M.B.,
657 Almendinger, J.E., Strock, K.E., Van der Meulen, D., Elias, J.E., Saros, J.E., 2016.
658 Nitrogen deposition to lakes in national parks of the western Great Lakes region: Isotopic
659 signature, watershed retention, and algal shifts. *Glob. Biogeochem. Cycles* 30, 514–533.

660 Husson, F., Josse, J., Le, S., Mazet, J., 2016. Multivariate exploratory data analysis and data
661 mining. R package (R Core Team).

662 Inglis, G.N., Bhattacharya, T., Hemingway, J.D., Hollingsworth, E.H., Feakins, S.J., Tierney, J.E.,
663 2022. Biomarker approaches for reconstructing terrestrial environmental change. *Annu.*
664 *Rev. Earth Planet. Sci.* 50, 1.

665 Jongejans, L.L., Mangelsdorf, K., Schirrmeister, L., Grigoriev, M.N., Maksimov, G.M.,
666 Biskaborn, B.K., Grosse, G., Strauss, J., 2020. *n*-Alkane Characteristics of Thawed
667 Permafrost Deposits Below a Thermokarst Lake on Bykovsky Peninsula, Northeastern
668 Siberia. *Front. Environ. Sci.* 8, 118.

669 Juggins, S., 2020. Rioja: analysis of quaternary science data. R package version (0.9-26). Available
670 from: <https://cran.r-project.org/package=rioja>

671 Junk, W.J., An, S., Finlayson, C.M., Gopal, B., Kvet, J., Mitchell, S.A., Mitsch, W.J., Robarts,
672 R.D., 2013. Current state of knowledge regarding the world's wetlands and their future
673 under global climate change: a synthesis. *Aquat. Sci.* 75, 151–167.

674 Kadetova, A.V., Radziminovich, Y.B., 2014. The catastrophic flood in Transbaikalia (Central
675 Asia) in 1897: a case study. *Nat. Hazards* 72, 423–441.

676 Koski-Vahala, J., Hartikainen H., Tallberg, P., 2001. Phosphorus mobilization from various
677 sediment pools in response to increased pH and silicate concentration. *J. Environ. Qual.* 30,
678 546–552.

679 Levi, E.E., Bezerci, G., Cakiroglu, A.I., Turner, S., Bennion, H., Kernan, M., Jeppesen E.,
680 Beklioglu, M., 2016. Multi-proxy palaeoecological responses to water level fluctuations in
681 three shallow Turkish lakes. *Palaeogeogr. Palaeoclimatol. Palaeoecol.* 449, 553–566.

682 Li, Z., Sun, Y., Nie, X., 2020. Biomarkers as a soil organic carbon tracer of sediment: Recent
683 advances and challenges. *Earth-Sci. Rev.* 208, 103277.

684 Liu, M., Ji, C., Hu, H., Xia, G., Yi, H., Them II, T.H., Sun, P., Chen, D., 2021. Variations in
685 microbial ecology during the Toarcian Oceanic Anoxic Event (Early Jurassic) in the
686 Qiangtang Basin, Tibet: Evidence from biomarker and carbon isotopes *Palaeogeogr.*
687 *Palaeoclimatol. Palaeoecol.* 580, 110626.

688 Luoto T.P., Kuhry, P., Holzkamper, S., Solovieva, N., Self, A.E., 2017. A 2000-year record of
689 lake ontogeny and climate variability from the north-eastern Russian Arctic. *Holocene* 27,
690 339–348.

691 Marzi, R., Torkelson, B.E., Olson, R.K., 1993. A revised carbon preference index. *Org. Geochem.*
692 20, 1303–1306.

693 Meyers, P.A. 2003. Applications of organic geochemistry to paleolimnological reconstructions: a
694 summary of examples from the Laurentian Great Lakes, *Org. Geochem.* 34, 261–289.

695 Meyers, P.A., Teranes, J.L., 2001. Sediment organic matter. In: *Tracking Environmental change*
696 *using lake sediments. Physical and Geochemical Method.* Last, V.M., Smol, J.P., (eds.).
697 Kluwer Academic Publishers, Dordrecht, The Netherlands.

698 Mitsch, W.J., Gosselink J.G., 2007. Wetlands, 4th Edition. Wiley & Sons, United States of
699 America.

700 Nadmitov, B., Hong, S., Kang, S.I., Chu, J.M., Gomboev, B., Janchivdorj, L., Lee, C-H., Khim,
701 J.S., 2015. Large-scale monitoring and assessment of metal contamination in surface water
702 of the Selenga River basin (2007-2009). *Environ. Sci. Pollut. Res.* 22, 2856–2867.

703 Orlov, A.P., 1872. General remarks on earthquakes, with special reference to South Siberia and
704 Turkestan Region. *Proceedings of the Kazan University Society of Natural Sciences* 3, 1–
705 10.

706 Pancost, R.D., Boot, C.S., 2004. The palaeoclimatic utility of terrestrial biomarkers in marine
707 sediments. *Mar. Chem.* 92, 239–261.

708 Peters, K.E., Moldowan, J.M., 1993. *The Biomarker Guide*. Prentice-Hall, Englewood Cliffs.

709 Peters, K.E., Walters, C.C., Moldowan, J.M., 2005. *The Biomarker Guide, Volumes 1 and 2:*
710 *Biomarkers and Isotopes in Petroleum Exploration and Earth History*, 2nd edition.
711 Cambridge University Press, USA, pp. 616–617.

712 Pinegin, A.V., Rogozin, A.A., Leshchikov, F.N., Kulish, L.Y., Yakimov, A.A., 1976. Shore
713 dynamics of Lake Baikal at the new level regime. Nauka, Moscow.

714 Pisarsky B.I., Hardina A.M., Naganawa H., 2005. Ecosystem evolution of Lake Gusinoe
715 (Transbaikal Region, Russia). *Limnology* 6, 173–182.

716 Plyusnin, A.M., Kislitsina, L.B., Zhambalova, D.I., Peryazeva, E.G., Udodov, Y.N., 2008.
717 Development of the chemical characteristics of ground water at the Delta of the Selenga
718 River. *Geochem. Int.* 46, 288–295.

719 Potasznik A., Szymczyk, S., 2015. Magnesium and calcium concentrations in the surface water
720 and bottom deposits of a river-lake system. *J. Elem.* 20, 677–692.

721 Poynter, J., Eglinton, G., 1990. Molecular composition of three sediments from Hole 717C: the
722 Bengal Fan. In: Cochran, J.R., Stow, D.A.V., *Proc. ODP Sci. Results.* 116, 155–161.

723

724 Ramsar. 2022. The 4th strategic plan 2016-2024: The convention on wetlands of international
725 importance especially as waterfowl habitat – the “Ramsar Convention”. [online] Available
726 from: <http://www.ramsar.org/about/the-ramsar-convention-and-its-mission>. [Accessed:
727 March, 2022].

728 Reuss, N., Conley D.J., 2005. Effects of sediment storage conditions on pigment analyses. *Limnol.*
729 *Oceanogr. Methods* 3, 477–487.

730 Robinson, W.P., Anosova, G.B., 2004. Mining and mineral development management policy in
731 the Selenga River watershed. In: *Science for watershed conservation: multidisciplinary*
732 *approaches for natural resource management Conference, Ulan-Ude, Russia and*
733 *Ulanbaatar, Mongolia.*

734 Rullkötter, J., 2000. Organic matter: The driving force for early diagenesis. In Schulz, H. D. & M.
735 Zabel (ed.) *Marine Geochemistry*. Springer Verlag, Berlin. pp. 129–172.

736 Russell, M., Rosell-Melé, A., 2005. Preliminary study of fluxes of major lipid biomarker classes
737 in the water column and sediments of Lake Baikal, Russia. *Glob. Planet. Change* 46, 45–
738 56.

739 Sachse, D., Radke, J., Gleixner, G., 2006. δD values of individual n-alkanes from terrestrial plants
740 along a climatic gradient – implications for the sedimentary biomarker record. *Org.*
741 *Geochem.* 37, 469–483.

742 Sayer, C.D., Burgess, A., Kari, K., Davidson, T.A., Peglar, S., Yang, H., Rose, N., 2010. Long-
743 term dynamics of submerged macrophytes and algae in a small and shallow, eutrophic lake:
744 implications for the stability of macrophyte-dominance. *Freshw. Biol.* 55, 565–583.

745 Schefuß, E., Rattmeyer, V., Stuut, J.-B.W., Jansen, J.H.F., Sinninghe Damsté, J.S., 2003. Carbon
746 isotope analyses of n-alkanes in dust from the lower atmosphere over the central eastern
747 Atlantic. *Geochim. Cosmochim. Acta* 67, 1757–1767.

748 Scholz C.A., Hutchinson D.R., 2000. Stratigraphic and structural evolution of the Selenga Delta
749 Accommodation Zone, Lake Baikal Rift, Siberia. *Int. J. Earth. Sci.* 89, 212–228.

750 Sievers, M., Hale, R., Parris, K.M., Swearer, S.E., 2018, Impacts of human-induced environmental
751 change in wetlands on aquatic animals. *Biol. Rev.* 93, 529–554.

752 Silliman, J.E., Meyers, P.A., Bourbonniere, R.A., 1996. Record of postglacial organic matter
753 delivery and burial in sediments of Lake Ontario. *Org. Geochem.* 24, 463–472.

754 Sokal, M.A., Hall, R.I., Wolfe, B.B., 2010. The role of flooding on inter-annual and seasonal
755 variability of lake water chemistry, phytoplankton diatom communities, and macrophyte
756 biomass in the Slave River Delta (Northwest Territories, Canada). *Ecohydrology* 3, 41–54.

757 Summers, J.C., Kurek J., Ruhland, K.M., Neville, E.E., Smol J.P., 2017. Assessment of multi-
758 trophic changes in a shallow boreal lake simultaneously exposed to climate change and
759 aerial deposition of contaminants from the Athabasca Oil Sands Region, Canada. *Sci. Total*
760 *Environ.* 592, 573–583.

761 Tarasov, P.E., Müller, S., Zech, M., Andreeva, D., Diekmann, B., Leipe, C., 2013. Last glacial
762 vegetation reconstructions in the extreme-continental eastern Asia: Potentials of pollen and
763 *n*-alkane biomarker analyses. *Quat. Int.* 290–291, 253–263.

764 Tissot, B.P., Welte, D.H., 1978. Petroleum formation and occurrence, Springer-Verlag, Berlin
765 Heidelberg, Germany. pp. 643–644.

766 Tolosa, I., Mora, S., Reza, M., Villeneuve, J., Bartocci, J., Cattini, C., 2004. Aliphatic and aromatic
767 hydrocarbons in coastal Caspian Sea sediments. *Mar. Pollut. Bull.* 48, 44–60.

768 Vogts, A., Schefuss, E., Badewien, T., Rullkoetter, J. 2012. *n*-Alkane parameters from a deep sea
769 sediment transect off southwest Africa reflect continental vegetation and climate
770 conditions. *Org. Geochem.* 47, 109–119.

771 Volkman, J.K., Revill, A.T., Holdsworth, D.G., Fredericks, D., 2008. Organic matter sources in
772 an enclosed coastal inlet assessed using lipid biomarkers and stable isotopes. *Org.*
773 *Geochem.* 39, 689–710

774 Vologina, E.G., Kalugin, I.A., Osukhovskaya, Y.N., Sturm, M., Ignatova, N.V., Radziminovich,
775 Y.B., Dar'in, A.V., Kuz'min, M.I., 2010. Sedimentation in Proval Bay (Lake Baikal) after
776 earthquake-induced subsidence of part of the Selenga River delta. *Russ. Geol. Geophys.*
777 51, 1275–1284.

778 Wasserman, R.J., Dalu, T., 2022. Tropical freshwater wetlands: an introduction. In: *Fundamentals*
779 *of tropical freshwater wetlands: from Ecology to Conservation Management* 1–22.
780 Elsevier.

781 Wisnieski, E., Ceschim, L.M.M., Martins, C.C., 2016. Validação de um método analítico para
782 determinação de marcadores orgânicos geoquímicos em amostras de sedimentos marinhos.
783 *Quim. Nova* 39, 1007–1014.

784 Wu, Y., Wen, Y., Zhou, J., Wu, Y., 2014. Phosphorus release from lake sediments: effects of pH,
785 temperature, and dissolved oxygen. *J. Civ. Eng.* 18, 323–329.

786 Yang, H.J., Lee, C.J., Chiang, Y.J., Jean, J.S., Shau, Y.H., Takazawa, E., Jiang W.T., 2016.
787 Distribution and hosts of arsenic in a sediment core from the Chianan Plane in SW Taiwan:
788 Implications on arsenic primary source and release mechanisms. *Sci. Total Environ.* 569,
789 212–222.

790 Yunker, M.B., Macdonald, R.W., Vingarzan, R., Mitchell, R.H., Goyette, D., Sylvestre, S., 2002.
791 PAHs in the Fraser River basin: a critical appraisal of PAH ratios as indicators of PAH
792 source and composition. *Org. Geochem.* 33, 489–515.

Table 1. *n*-Alkane ratios used in the literature to distinguish the different sources of organic matter (OM).

Name		<i>n</i> -Alkane equations	Diagnostic values	Source assignment	References
Odd/Even ratios	O/E (< C ₂₄)	$\frac{\sum \text{odd } C_{11}-C_{23}}{\sum \text{even } C_{10}-C_{22}}$	~ 1.0	petroleum and their by-products	Tolosa et al. (2004)
	O/E (> C ₂₃)	$\frac{\sum \text{odd } C_{25}-C_{37}}{\sum \text{even } C_{24}-C_{36}}$	>> 1.0	biogenic origin	
Carbon Preference Index	CPI ₁	$0.5^* \frac{(n-C_{15}+n-C_{17}+n-C_{19}+n-C_{21}+n-C_{23})}{(n-C_{14}+n-C_{16}+n-C_{18}+n-C_{20}+n-C_{22})} + \frac{(n-C_{15}+n-C_{17}+n-C_{19}+n-C_{21}+n-C_{23})}{(n-C_{16}+n-C_{18}+n-C_{20}+n-C_{22}+n-C_{24})}$	≤ 1.0	anthropogenic and/or reworked material	Bray and Evans (1961) Aboul-Kassim and Simoneit (1996)
	CPI ₂	$0.5^* \frac{(n-C_{25}+n-C_{27}+n-C_{29}+n-C_{31}+n-C_{33})}{(n-C_{24}+n-C_{26}+n-C_{28}+n-C_{30}+n-C_{32})} + \frac{(n-C_{25}+n-C_{27}+n-C_{29}+n-C_{31}+n-C_{33})}{(n-C_{26}+n-C_{28}+n-C_{30}+n-C_{32}+n-C_{34})}$	1.0 – 3.0	aquatic OM contribution	
Terrestrial-to-Aquatic Ratios	TAR	$\frac{n-C_{25}+n-C_{27}+n-C_{29}+n-C_{31}+n-C_{33}}{n-C_{15}+n-C_{17}+n-C_{19}+n-C_{21}+n-C_{23}}$	>> 1.0	terrestrial OM contribution	Bourbonniere and Meyers (1996) Silliman et al. (1996) Chevalier et al. (2015)
			< 1.0	autochthonous contribution	
Aquatic Proxies	P _{aq wax}	$\frac{n-C_{23}+n-C_{25}}{n-C_{23}+n-C_{25}+n-C_{27}+n-C_{29}}$	< 0.1	allochthonous OM	Ficken et al. (2000) Li et al. (2020)
			0.1 - 0.4	mixed sources	
Average Chain Length ratios	ACL	$\frac{27 * (n-C_{27}) + 29 * (n-C_{29}) + 31 * (n-C_{31}) + 33 * (n-C_{33}) + 35 * (n-C_{35})}{n-C_{27}+n-C_{29}+n-C_{31}+n-C_{33}+n-C_{35}}$	> 0.4	autochthonous OM, typically submerged and floating macrophytes	Poynter and Eglinton (1990) Freeman and Pancost (2014) Sachse et al. (2006) Vogts et al. (2012)
			27 – 28	predominance of vascular plant	
			28 – 29	contribution of trees/shrubs	
Isoprenoids and short <i>n</i> -alkanes ratios	Pri/Phy	$\frac{\text{Pristane}}{\text{Phytane}}$	< 1	anoxic conditions	Tissot and Welte (1978) Didyk et al., 1978 Peters et al. (2005)
			> 3	oxic conditions	
	Pri/ <i>n</i> -C ₁₇	$\frac{\text{Pristane}}{n-C_{17}}$	< 1	increase on biodegradation of <i>n</i> -alkanes	Peters and Moldowan (1993)
Phy/ <i>n</i> -C ₁₈	$\frac{\text{Phytane}}{n-C_{18}}$	> 3	increase in the delivery of phototrophic OM	Commendatore and Esteves (2004)	

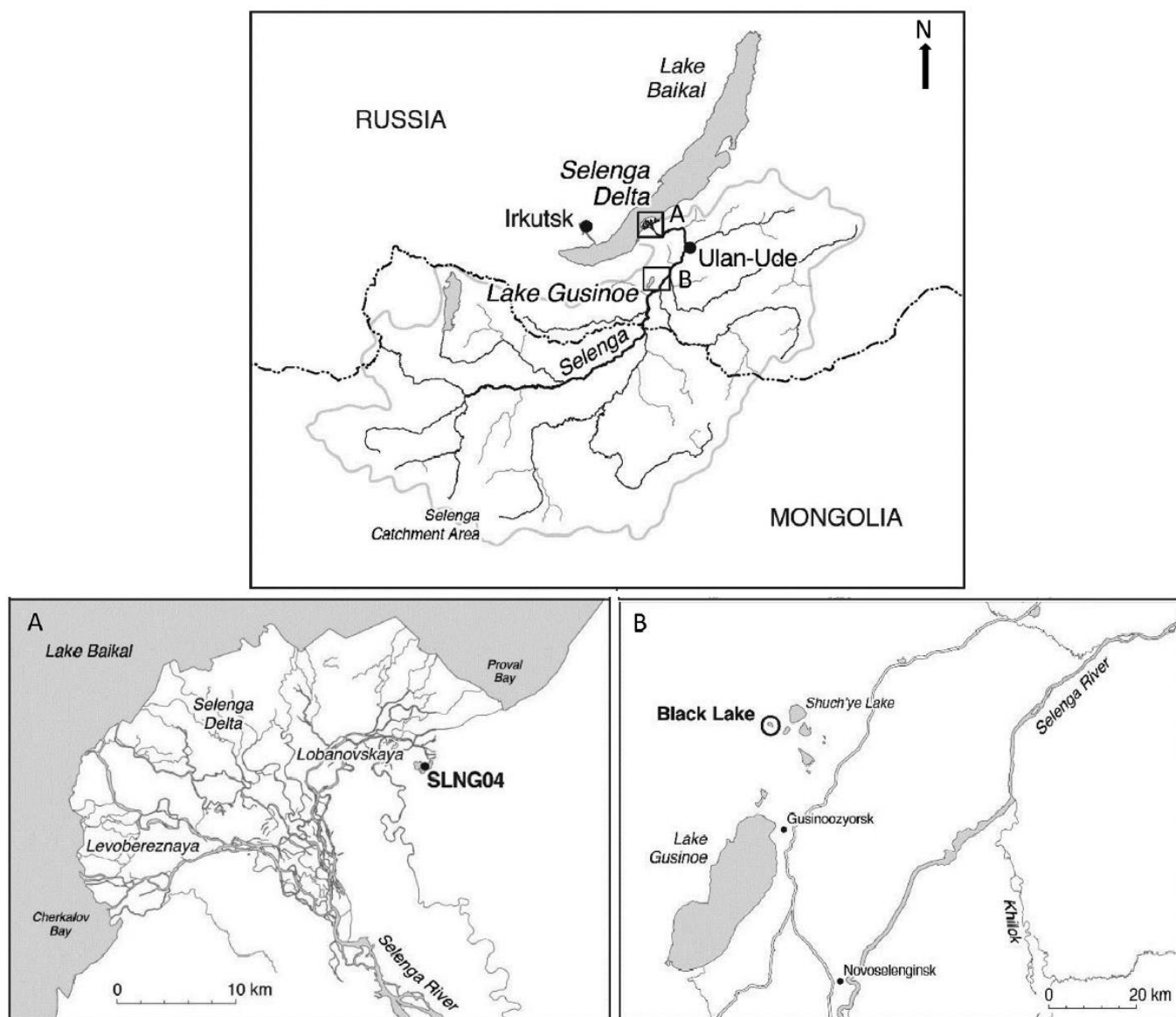


Fig. 1. Map of the Selenga River basin in southeast Siberia and northern Mongolia, with major river tributaries and cities labelled. Subset A. Map of the Selenga Delta with SLNG04 location indicated. Subset B. Location of Black Lake (BRYT02 site) in the Gusinoozersk region (adapted from Adams et al. 2018).



Fig. 2. Shallow lakes studied in Selenga River basin. Subset A: SLNG04 lake, view from open water, facing southeast; Subset B: SLNG04 view from shore, facing northwest; Subset C: BRYT02 view from the eastern shore, facing northwest; Subset D: Black Lake (BRYT02 site) view from the southeastern shore, facing west.

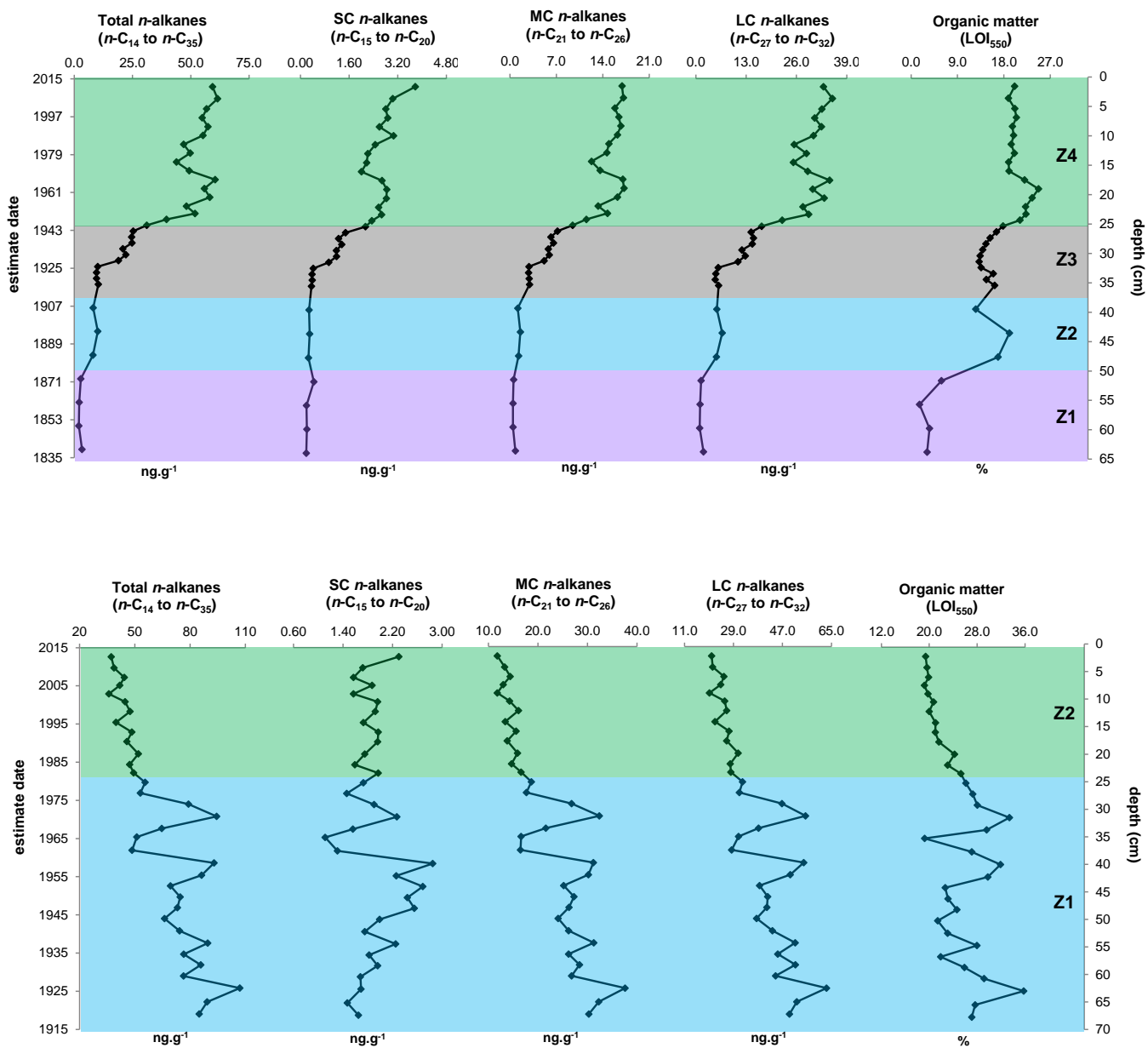


Fig. 3. Profiles of total, short-chain (SC), mid-chain (MC) and long-chain *n*-alkanes (LC) (in $\mu\text{g g}^{-1}$) and organic matter content (LOI_{550} , in %) for the sediments from SLNG04B and BRYT02B cores.

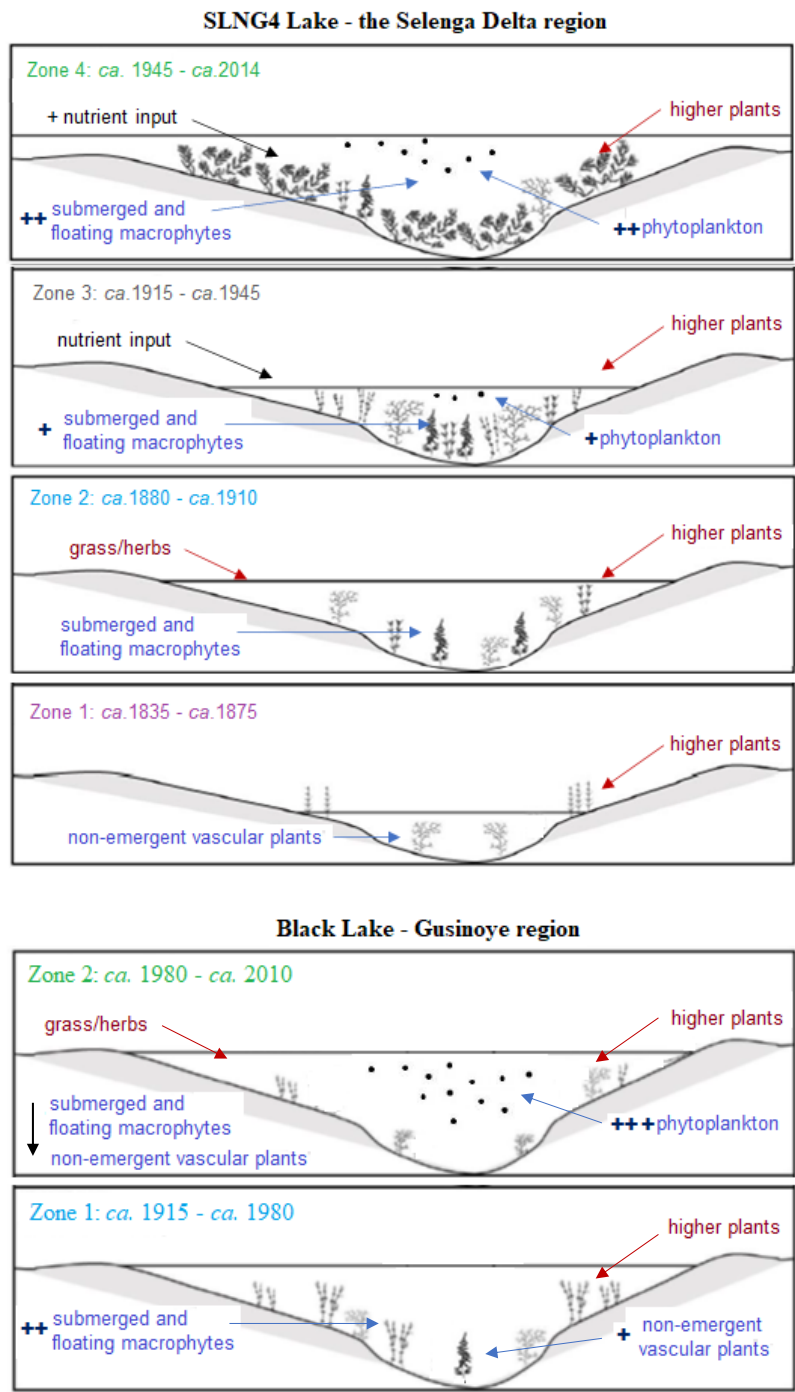


Fig. 4. Conceptual diagram of ecological community change at SLNG04 and Black Lakes since the late-19th and early-20th, respectively.

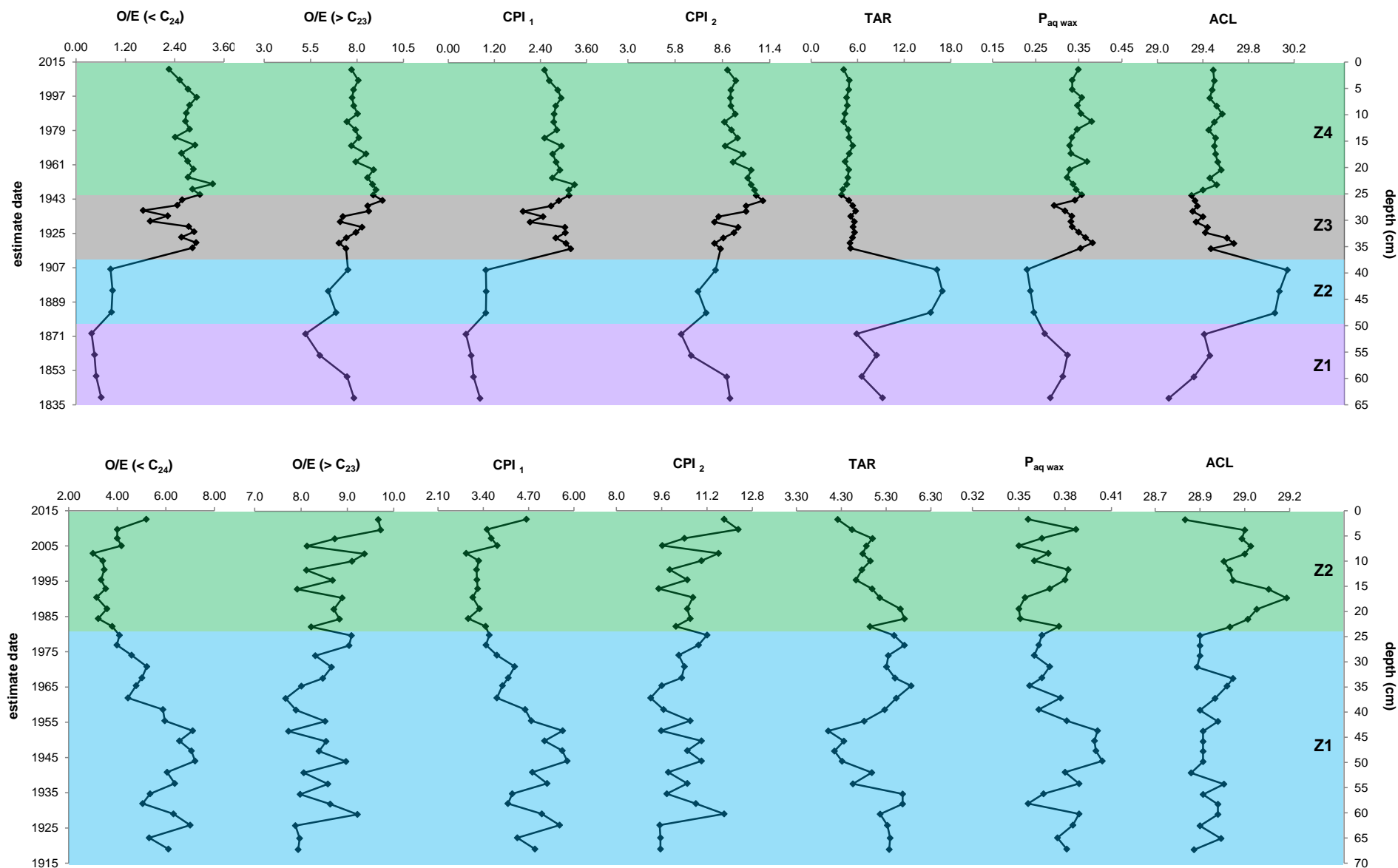


Fig. 5. Profiles of selected *n*-alkane indices for the sediments from SLNG04B and BRYT02B cores: odd/even (O/E < C₂₄ and O/E > C₂₃), carbon preference index considering short-chain *n*-alkanes (CPI₁), and long-chain *n*-alkanes (CPI₂), terrestrial over aquatic (TAR), the P_{aq wax}, and average chain length (ACL) ratios.

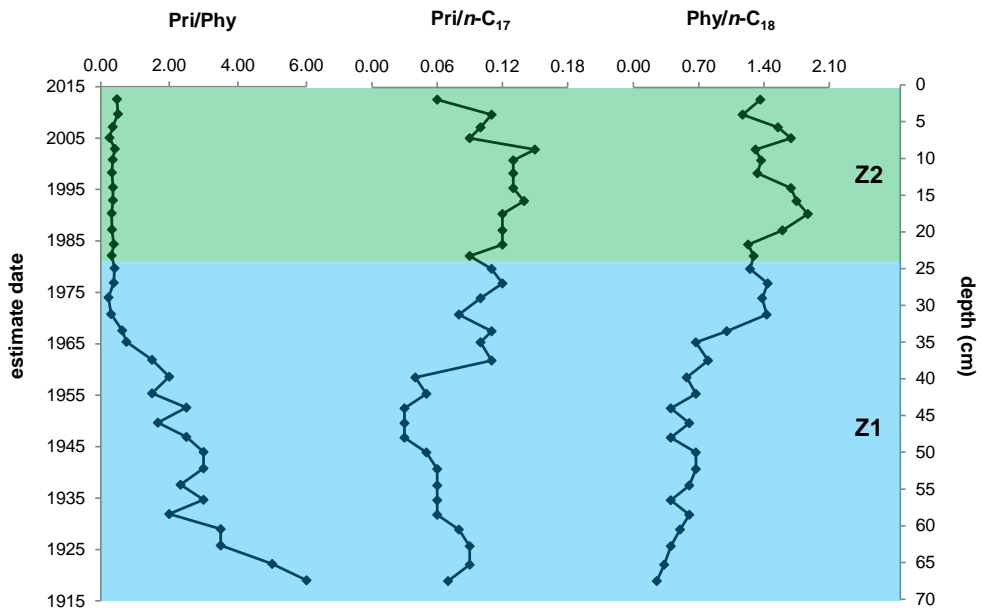
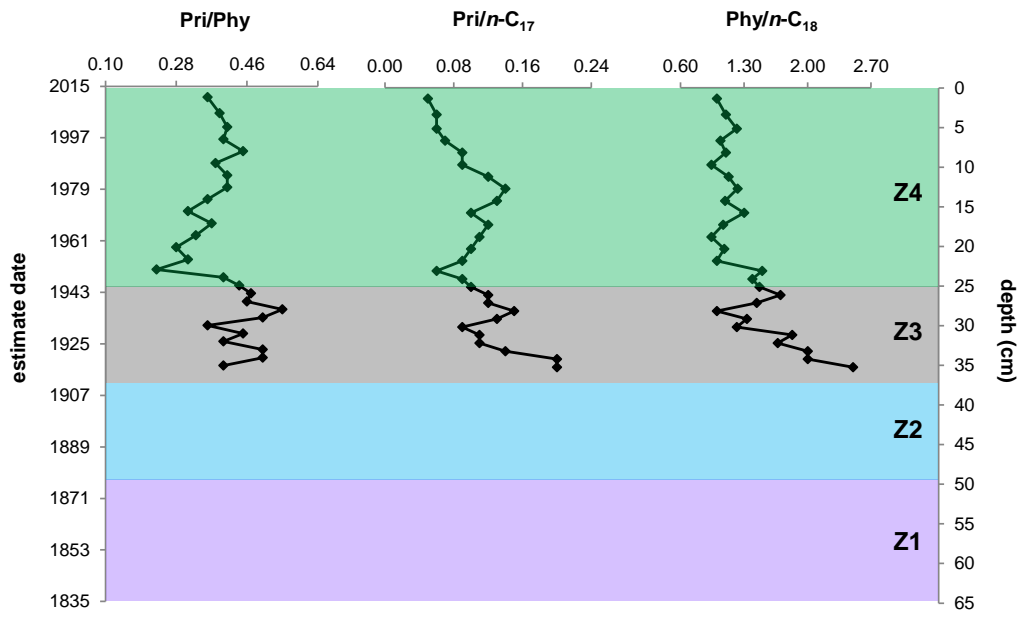
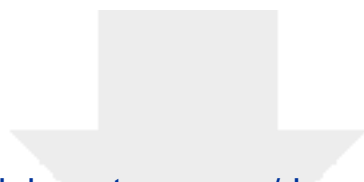


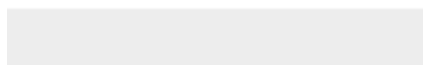
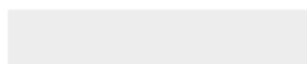
Fig. 6. Profiles of isoprenoid indices for the sediments from SLNG04B and BRYT02B cores: pristane/phytane (Pri/Phy), pristane/*n*-C₁₇ (Pri/ *n*-C₁₇), and phytane/*n*-C₁₈ (Phy/ *n*-C₁₈) ratios.



Click here to access/download

Supplementary Material

Sup Info_Alkanes Selenga FINAL.docx



Declaration of interests

Title: Earthquake, floods and changing land use history: a 200-year overview of environmental changes in southern Siberia as indicated by n-alkanes and related proxies in sediments from shallow lakes

Authors: César C. Martins, Jennifer K. Adams, Handong Yang, Alexander A. Shchetnikov, Maikon Di Domenico, Neil L. Rose, Anson W. Mackay

The authors declare that they have no known competing financial interests or personal relationships that could have appeared to influence the work reported in this paper.

The authors declare the following financial interests/personal relationships which may be considered as potential competing interests:

* Prof. Dr. César de Castro Martins
Centro de Estudos do Mar, UFPR, Brazil
<http://orcid.org/0000-0002-2515-5565>

CRedit author statement

César C. Martins: Conceptualization; Data curation; Formal analysis; Visualization; Writing - original draft; Writing - review & editing. **Jennifer Adams:** Conceptualization; Data curation; Writing - review & editing. **Handong Yang:** Formal analysis; Writing – review & editing. **Alexander A. Shchetnikov:** Conceptualization; Project administration; Resources. **Maikon Di Domenico:** Formal analysis; Writing – review & editing. **Neil Rose:** Conceptualization; Supervision; Writing – review & editing. **Anson W. Mackay:** Conceptualization; Supervision; Project administration; Resources; Writing – review & editing.